HSPI The Open Access Publisher

ABSE ANNALS OF BIOMEDICAL SCIENCE AND ENGINEERING
ISSN 2833-518X

Research Article

Enlarged Curvature, Torsion and Torque in Helical Conformations and the Stability and Growth of α-Peptide under the Isochoric and Isobaric Conditions: Variatonal Optimization

Tarik Omer Ogurtani*

Department of Metallurgical and Materials Engineering, Middle East Technical University, Ankara 06531, Turkey

More Information

***Address for correspondence:**
Tarik Omer Ogurtani, Department of Metallurgical and Materials Engineering, Middle East Technical University, Ankara 06531, Turkey,
Email: ogurtani@alumni.stanford.edu; ogurtani@metu.edu.tr

Submitted: September 30, 2024
Approved: October 05, 2024
Published: October 07, 2024

How to cite this article: Ogurtani TO. Enlarged Curvature, Torsion and Torque in Helical Conformations and the Stability and Growth of α-Peptide under the Isochoric and Isobaric Conditions: Variatonal Optimization. Ann Biomed Sci Eng. 2024; 8(1): 039-058. Available from: https://dx.doi.org/10.29328/journal.abse.1001032

Keywords: α-Peptide; Helical Conformation; Stability; Torsion, Torque; Skew symmetric Tensor

Check for updates

OPEN ACCESS

Abstract

The torsional deformation behavior of an elastic bar with a circular cross-section was investigated by applying invariant dyadic analysis, where the small finite displacement functions advocated by Saint-Venant (1855) were fully employed. It was found that the previously overlooked circumferential shear force field generated by pure torsion on the side walls of a bar produces an unusual torque term induced by the skew-symmetric part of the deformation tensor and exhibits quadratic length dependence along the z-axis of the bar. The adaptation of this torque term for a helical conformation of α-peptides creates moments acting on the circular cross-sections and is directed along the surface normal of circular cross-sections, which coincides with the tangent vector of the helix. The projection of this torque along the z-axis of the helix varies quadratically with the azimuthal angle. The radial component of the unusual torque, which also lies along the principal normal vector of the helix, starts to perform a precession motion by tracking a spiral orbit around the z-axis, whereas its apex angle decreases asymptotically with the azimuthal angle and finally reaches a finite value depending on the height of the helix along the z-axis. The ordinary torque terms, which are also deduced from the self- and anti-self-conjugate parts of the deformation tensor, have magnitudes half that of the full torque term reported in the literature. The present results were applied to the helical conformation of α-peptides designated by $\{3.6_{11}\}$ to show that the mechanical stability of strained open-ended helical conformations can be successfully achieved by spontaneous readjustments of the surface and bulk Helmholtz free energies under isothermal isochoric conditions. It has been demonstrated that the main contribution to the mechanical stability of α-peptide 3.6_{11} cannot come alone from the electrostatic dipole-dipole interaction potential of the anti-align excess dipole pairs but also from the surface Helmholtz free energy, which is characterized by a binding free energy of -15.5 eV/molecule (-32.56 Kcal/mole) for an alpha-peptide composed of 11 amino acid residues with a critical arc length of approximately 10 nm, assuming that the shear modulus is G = 1GPa and the surface Helmholtz specific free energy density is fs = 800 erg/cm^2. This result was in excellent agreement with the experimental observations of the AH-1 conformation of (Glu)n Cys at pH 8. The present theory indicates that only two excess permanent anti-align dipole pairs for one α-Helical peptide molecule is requirement to stabilize the whole secondary structure of the protein that is exposed to heavy torsional deformation during the folding processes which amounts to 7.75 eV/molecule stored electrostatic energy compared to the interfacial Helmholtz free energy of -23.25 eV/molecule, which is exposed to hydrophobic environments.

Nomenclature

$\varphi = \theta\ell \sim \theta z$: Relative twist rotation of the cross-sections; $\theta = \mathrm{d}\varphi / \mathrm{d}\ell$: Torsion angle, This is also denoted by "λ". It is a constant; $\vec{\varphi} = \theta z\hat{k}$: Twist angle of cross-sections of bar about z-axis; $d\vec{\varphi} = \theta dz\hat{k}$:Infinitesimal twist of two neighboring cross-sections distance dz; ϕ(*x,y*): Warping function; $\nabla\vec{s}$: Deformation dyadic (tensor); $\nabla\vec{s} = \dot{E}\{z(\hat{i}\hat{j} - \hat{j}\hat{i}) - \hat{k}\hat{i}\,y + \hat{k}\hat{j}\,x\}$: Displacement dyadic is given In Orthonormal three vectors set; $\vec{s} = \theta z(-\hat{i}\,y + \hat{j}x)$: displacement vector field for torsion; $\Phi = 1/2\left(\nabla\vec{S} + \vec{S}\nabla\right)$: Self-conjugate part (strain tensor); $\Psi = 1/2\left(\nabla\vec{S} - \vec{S}\nabla\right)$: Anti-self-conjugate part (strain tensor); $\Psi = -1/2\,I\times\left(\nabla\times\vec{S}\right)$: Implies vortex motion; $\vec{\omega} = 1/2\nabla\times\vec{S}$: Angular rotation vector. ½ curl $\vec{S}$; *mod* $\vec{\omega}$: The circular measure of rotation angle; $\vec{u} = -\vec{\omega}\times\vec{r}$: Displacement Rotation of a position vector; I: Idempotent or unit dyadic; $F^{\Psi}_{End}, F^{\Phi}_{End}$: Traction forces applied to the Free C-end; $F^{\Psi}_{Wall}, F^{\Phi}_{Wall}$: Traction forces applied to the sidewalls; $M^{\Psi}_{End}, M^{\Phi}_{End}$: Torque terms with respect to the Constrained-end cross sections; $M^{\Psi}_{Wall}(\ell), M^{\Psi}_{Wall}(L)$: Torque terms associated

with the Cylindrical side- walls force fields (i.e., an unusual torque term); $\hat{t}$: Local tangent vector of helix; $\hat{b}$: Binormal of helix; $d\hat{b}/d\ell = -\lambda\hat{n}$ "λ"Torsion of helix; λ=(1/R) *sin β cos β:* Torsion of simple helix; $d\hat{t}/d\ell = \kappa\hat{n}$: "*k*" curvature of helix; *β*: Inclination angle of helix; *R:* Radius of helix; $\vec{\theta} = d\vec{\varphi}/dl = \lambda\vec{t}$: $\vec{\theta}$ Vector describes the rate of variation of the twist Angle $\vec{\varphi}$ per unit arc length; $Mod\left[\vec{\theta}\right] = \lambda$: The torsion angle called by Landau & Lifshitz; *G:* Shear modulus or modulus of rigidity; *μ:* Mobility in the Einstein-Nernst equation; *a:* radius of the helical skeleton; ℓ : Arc length of the helical skeleton; *τ:* Relaxation time; $\nabla F_S^T(\ell)$: Surface Helmholtz free energy of helical form; $f_{s:}$ Specific Helmholtz surface free energy; $\nabla F_G(\ell)$: Global Helmholtz free energy; $\nabla F_B(\ell)$: Bulk Helmholtz free energy; $\delta\nabla F_S(\ell)$: Change in the surface Helmholtz free energy; $\nabla F_{Chem}(V)$: Chemical bulk Helmholtz free energy; $\nabla F_{Mech}(\ell)$: Mechanical bulk Helmholtz free energy; $\delta\nabla S_{In}$: Change in the internal entropy; $\delta\nabla F_G$: Change in the Helmholtz free energy; $\delta\nabla S_{Int}^G/\delta t = -1/T\delta\nabla F_G/\delta t \geq 0$: Planck (1887) criterion combined with the positive definite internal entropy hypothesis Isochoric isothermal changes for closed system; $\nabla F(a,\ell)$: Global Helmholtz function for extremum problem; $V_o(a,\ell)$: Volume of backbone skeleton; $\Sigma(a,\ell)$: Enlarged function for extremal solution; *x:* Lagrange Multiplier; ℓ^*, *a**: Stable arc length and radius; $E_{b:}$ Binding energy or extremal Helmholtz free for the Non-equilibrium stationary State; $\nabla F_G^* = -5.769$ *and* $\nabla G_G^* = +5.772$: Extremum values of Helmholtz and Gibbs energy Barriers for critical nucleation of α-peptide 3.6_{11}; $\ell^* = 0.59,0.56$: Critical nucleation arc length for the α-peptide 3.6_{11}; $\nabla F_M^B(\ell)$: Helmholtz free energy due to pure bending; M_b: Bending moment of amino acid skeleton; *E*: Young modulus of elasticity; v: ultrasonic longitudinal propagation velocity; ν: Poisson's ratio; ρ: Volumetric density; $\nabla F_{G:}$ Global Helmholtz free energy; ∇G_G: Global Gibbs free energy; $V_{d'-d}$: Dipole-dipole potential energy; d', *d:* Electrostatic dipole vectors; $\in_0$: Dielectric constant; $\vec{F}$: Force; *M*: Moment; C_ψ : Rotational rigidity due to the circumference Shear force field at the cylindrical wall; *I*: Section moment of inertia Dielectric constant; $\pm E_{d-d}(\ell)$: Interaction potential between dipole pairs Negative for Anti-align Positive for on-align pairs; δ: Variation operator; *x*: Lagrange Multiplier; $\Sigma(a,\ell)$: Lagrangian Function for the extremal solution; ℓ^*, *a**: Stable arc length and helical radius; ∇F_G^* : Binding free energy of the helical conformation; *M*: Angular moment of helix; *Q*: shear force; I: Moment of inertia; ω: Angular velocity of section along arc length; φ : Twist angle along the arc length; C_ψ : Rotational rigidity; Q: Shear

Introduction

In this work, we have to place special emphasis on the anti-self-conjugate part of the deformation tensor (dyadic) associated with a simple helical linear elastic body with circular cross-sections, which is exposed to pure torsional and bending moments. The re-examination of this historical problem related to the pure torsional deformation of a solid bar is important because of the underestimated role of the non-vanishing shear force field directed along the tangential orientation of the circumferences of the cylindrical sidewalls of the solid bars and helical conformations. Unfortunately, not only the shear surface force field but also the anti- self-conjugate part of the deformation tensor arising from the proposed pure torsional displacement fields by Saint-Venant [1] (1855) have been completely neglected in the literature [2-5]. These incidents have occurred repeatedly in the literature, mainly because while people are trying to find approximate solutions for the Airy differential equations associated with the stress function arising from the arbitrarily shaped cross-sections exposed to wrapping, they have intentionally adapted the free surface boundary conditions to simplify the approximate treatments of boundary value problems.

One can easily prove that the self-conjugate strain dyadic deduced from the deformation tensor obtained from the Saint-Venant displacement field can rigorously obey the compatibility requirements. This sidewall shear force field in the treatment of the skew-symmetric part of the deformation tensor appears to be rotational in character and can be represented by a torque term such as $\int dA\vec{F}\wedge\vec{r} \neq 0$ with respect to the center of mass (c.m.) of the circular cross-sections. In addition, these shear circumference forces owing to the circular symmetry of the cross-sections result in zero contribution $\int dA\vec{F} \Rightarrow 0$ to the global force balance equation, but not to the torque global balance. Therefore, it is necessary to consider the overlooked secondary facts in the complete treatment of this problem. The present results, when applied to the helical conformations of peptides in collaboration with the irreversible thermodynamics postulates, show that the stored or residual elastic deformation energy density due to the unusual new torque term can counteract the surface and/or the electrostatic monopolar and dipole–dipole interaction energies to create a mechanism for the desired absolute configurational stability of the helix with a critical size and binding free energy for a well –defined arc length under isothermal isochoric conditions. This phenomenological situation relies on the fundamental postulate that, which indicates that any increase in the Helmholtz surface free energy of an isochoric closed system by the enlargement of its surface area results in a simultaneous reduction in the stored elastic strain energy content of the body [6-8]. The validity of this hypothesis has also been rigorously justified by the formulation of the contributions of the electrostatic dipole–dipole interaction potential to the Helmholtz and Gibbs volumetric specific free energies, where the anti-align pairs [⇑⇓] enter into the scenario with negative and positive signs, respectively, for the isochoric and isobaric systems.

Electrostatic dipole-dipole interaction potential contribution for given helical peptide chain is directly proportional with the excess number of anti-align [⇑⇓] permanent dipole pairs -that are mostly present in the steroid

rings of the Peptide skeleton together with align- pairs [⇑⇓]- and generates a negative new term in the Global Helmholtz free energy balance equation in such way that its magnitude changes linearly with the arc length having a negative sign similar to the ordinary Helmholtz surface free energy. This is quite contrary to the alignment pairs because they enter the scenario with a positive sign, which inhibits mechanical stability under isochoric and isothermal conditions.

As a byproduct of the present theory, isobaric growth thermokinetics of the helical peptide conformation are formulated under torsional and bending deformation stress, which indicates that there is an activation Gibbs free energy barrier for the growth of critical nuclei that can only be surmounted by large thermal fluctuations. However, this situation can be mediated by an excess number of online [⇑⇓] dipole pairs created at elevated temperatures because of permanent dipole orientation switching through localized temperature fluctuations (local melting). This process reverses the contribution of electrostatic D-D interaction potential to the global Gibbs free energy.

Torsion of a circular bar

The torsional small displacements (twist) of a straight bar with arbitrary cross-sections were first introduced by Saint-Venant (1855) and later formulated by Timoshenko and Goodier [4] and Landau and Lifshitz [5], such as $u_x = -\Theta zy, u_y = \Theta zx$ and $u_z = \Theta\Psi(x,y)$. Where the cross-section warping function $\psi(x,y)$ is also discussed in detail and proven to be zero for circular cross-sections. When necessary, we used a cylindrical coordinate system, namely {r, θ, z}. Set $\{\hat{r}, \vec{r}\}$ denotes the unit and radial position vectors in the circular cross-sections, respectively. While maintaining the second author's universal vectorial expression for the infinitesimal rotation $\delta\vec{u} = \delta\vec{\varphi}\times\vec{r} \rightarrow\equiv \vec{s}$ formally [5], one may write down the relative torsional deformation of two neighboring cross-sections at a distance dz by $[d\vec{\varphi} = \Theta dz\hat{k}]$ where ϕ is the twist angle and Θ is the torsion angle which is the angle of rotation per unit length of the bar, namely Θ = $d\phi/dz$. If we assume that the torsion angle is constant, $\delta\Theta = 0$ for those cross-sections located at any distance z from the xy-reference plane, which is the undeformed z = o plane (origin) situated at the bottom or top ends of the bar and whose surface normal direction coincides with the z-axis, denoted by the $\hat{k}$ unit vector. The integration of the above expression from the origin z = 0 to any arbitrary point along the z-axis is denoted by z, which results in $\int_0^{\varphi} d\vec{\varphi} = \int_0^z dz\,\Theta\hat{k} \rightarrow \vec{\varphi} = \Theta z\hat{k}$. In the present case, the torsional deformation of the bar was approximately along the z-axis, which is indicated by $\hat{k}$. It can be proven that above the given vectorial equation for the infinitesimal format with the newly formulated argument, it may be transformed into $\vec{u} = (\Theta z\hat{k})\times\vec{r} \rightarrow\equiv \vec{s}$, and then may be evaluated exactly; $\vec{s} \equiv \vec{u} = \Theta z\,(\vec{k}\times\vec{r}) = \Theta z\left[-\hat{i}\,y + \hat{j}\,x\right]$ without making any approximation, such as the smallness of the torsion, provided that the torsion angle Θ remains constant. This torsional deformation causes the generators on the sides of the bar, which are initially parallel to its axis, to become circular simple helices in the form $\vec{r}(z) = R\{\cos, \sin, \cot\beta\}$ and cutting the generators at a constant inclination angle, denoted by β "torsion angle." where one has additional parameters, such as the twist angle $\theta = z\Theta$, and R is the radius of the circular bar [9].

Now, we have assumed that the torsion angle is very small but constant; therefore, one can use the heterogeneous small-strain theory of elasticity [10] for the further development of the torsional deformation theory using dyadic vector algebra. One may write the nonion form of the deformation dyadic exactly from the given displacements in dyad format $\nabla\vec{s} = \Theta\{z(\hat{i}\,\hat{j}\text{-}\hat{j}\,\hat{i}) - \hat{k}\,\hat{i}\,y + \hat{k}\,\hat{j}\,x\}$ where $\{\hat{i}, \hat{j}, \hat{k}\}$ is an orthonormal arbitrary set of three vectors, which is the choice of convenience attached to the circular cross-section of the bar in such a way that $\hat{k}$ k-unit vector acts as a surface normal vector of the clamped bottom end of the bar. We can easily form the self-conjugate $\Phi = 1/2\left(\nabla\vec{s} + \vec{s}\nabla\right)$ and anti-self-conjugate parts $\Psi = 1/2\left(\nabla\vec{s} - \vec{s}\nabla\right)$ of the strain dyadic. Where $\Phi = 1/2\left(\nabla\vec{s} + \vec{s}\nabla\right)$ is the small-displacement vector field. They may be clearly represented by the matrix or nonion format because the components are explicitly given through the displacement functions.

$$\Phi = 1/2\begin{bmatrix} 0 & 0 & -\Theta y \\ 0 & 0 & \Theta x \\ -\Theta y & \Theta x & 0 \end{bmatrix},\quad \psi = 1/2\begin{bmatrix} 0 & 2\Theta z & \Theta y \\ -2\Theta z & 0 & -\Theta x \\ -\Theta y & \Theta x & 0 \end{bmatrix} \quad (1)$$

Where the first dyadic corresponds to so-called strain tensor, which is symmetric and can be proven [10] that it satisfies the compatibility conditions for the uniqueness of the static elastic equilibrium solutions, $\nabla\times\Phi\times\nabla = 0$ [10,11]. The second dyadic corresponds to a skew-symmetric part of the deformation dyadic called the anti-self-conjugate. One can show that This skew-symmetric dyadic may be written as $\Psi = -1/2\,I\times\left(\nabla\times\vec{s}\right)$, which implies that there is a vortex motion represented by the angular rotation vector $\vec{\omega} = 1/2\nabla\times\vec{s}$ = [1/2 curl $\vec{s}$] whose circular measure is *mod* $\vec{W}$. Here, the rotation is represented by $d\vec{u} = -\vec{\omega}\times d\vec{r}$ for a small displacement in the vicinity of the origin. Here, I is an idempotent or unit dyadic, which has a nonion form $I = \hat{i}\,\hat{i} + \hat{j}\,\hat{j} + \hat{k}\,\hat{k}$. Because all the components are shear in character, the connection between the deformation and stress dyadic for an isotropic elastic solid involves only a single scalar constant, which is the shear modulus of elasticity or modulus of rigidity denoted by G [2]. Therefore, we can perform all operations using the deformation tensor symbolically, and at the end multiplied by G as shown in Figure 1 explicitly, we obtain the results in terms of torque or force with proper dimensions. In our formulations, we only use two static mechanical equilibrium conditions for a rigid body because the strain tensor already satisfies the compatibility conditions necessary for the uniqueness of the elastic solutions, which are the global force and torque balance equations, [11] respectively, are given by:

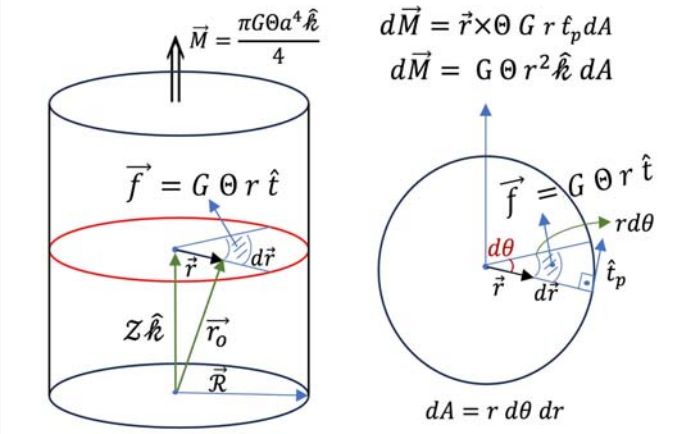

Figure 1: Shows the vectorial geometric connections employed in the computation of the global force $\vec{f}_r = G(\hat{k}.(\Phi+\Psi))$ and torque terms $d\vec{M} = G\,\Theta(\vec{r}) \times (\hat{k}.(\Phi+\Psi))$ associated with the self and anti-self-conjugate deformation tensors for circular cross-sections of cylindrical bar. Note: G shear modulus and it should be included in the force and torque formulas.

$$G\int_{End} \hat{k}.(\Phi+\Psi)dA + G\int_{Wall} \hat{r}.(\Phi+\Psi)dS + \int \rho \vec{F} dV + \vec{F}_{FixEnd} = 0$$

Force (2)

And

$$G\int_{End} \vec{r} \times \left(\hat{k}.(\Phi+\Psi)\right) dA + G\int_{Wall} (\vec{r}+z\hat{k}) \times \left(\hat{r}.(\Phi+\Psi)\right) dS + \int \rho \vec{r}_0 \times \vec{F} dV + M_{FixEnd} = 0.$$

Torque (3)

Here, $dA = r\, d\theta\, dr$ and $dS = a\, d\theta\, dz$ are infinitesimal areas selected for the integration procedures, associated with the top free-end cross sections and side walls of the bar, are demonstrated clearly in Figures 1,2 using blue and red crossed-hatchet areas. In the global upper free- end torque $\vec{M}$ expression as illustrated in Figure 1a, the radius of the bar is given by a; $\vec{r} = (\hat{i}x + \hat{j}y)$ is the polar coordinate of the variable point on the cross-section, and z is the distance of the cross-section from the bottom clamp end of the bar. $(\vec{r}_O = \vec{r} + z\hat{k})$ is the position vector of any point in the body of the bar, as well as on the sidewall surfaces of a circular cylindrical bar.

These expressions include not only the surface tractions (forces and moments), but also the body forces denoted by $\rho\vec{F}$. For the torque calculations associated with the side-wall forces in a given cross-section, the bottom end is taken as the reference plane and its centroid as the origin. In the present case, we have no body forces because, as usual, gravitational, electrostatic, or magnetic fields are omitted following practice, but we have implicit forces and moments owing to rigidly holding the bottom end of the bar. These constraints can be easily evaluated by computing the other terms in the above equations explicitly and directly from known deformation tensor components. As we will show, the total force arising from the deformation tensor is zero, and the value of the total torque is independent of the choice of origin [12] means that we can take the centroid of each cross-section as an origin, and the position vector may be denoted by radial vector. Traction forces should be applied to the free C-end F^{Ψ}_{End}, F^{Φ}_{End}, (Figure 1) and the side walls F^{Ψ}_{Wall}, F^{Φ}_{Wall}, (Figure 2) to balance the forces arising from the self- and anti-self-conjugate parts of the deformation dyadic, which can be calculated as follows:

$$F^{\Psi}_{End} = G\int \hat{k}.\Psi dA = 1/2G\Theta \int (\hat{j}x - \hat{i}y)\, dA = 1/2G\Theta\hat{k} \times \int \vec{r} dA \Rightarrow 0 \quad (4)$$

And

$$F^{\Phi}_{End} = G\int \hat{k}.\Phi dA = 1/2G\Theta \int (\hat{j}x - \hat{i}y)\, dA = 1/2G\Theta\hat{k} \times \int \vec{r} dA \Rightarrow 0 \quad (5)$$

The traction surface forces acting on the free end of the bar drop out because the first areal moment of a circular cross-section with respect to the center of gravity becomes zero because of symmetry. One obtains a zero contribution for the sidewall if one uses the self-conjugate part, because $\hat{r} \cdot \Phi = 0$ [11]. However, the shear-type traction force density acting on the side walls along the tangent direction $\hat{t} = \hat{k} \times \hat{r}$ of the circumferences is given by $\hat{r} \cdot \Psi = -1/2\, \hat{r} \cdot (I \times (\nabla \times s)) = -1/2\, \hat{r} \times (\nabla \times s)) = (\Theta z\, \hat{k} \times \hat{r}) = \Theta z \hat{t}$. This is owing to the anti-self-conjugate part of the deformation dyadic, and it is nonvanishing locally $(\Theta z\hat{t} = \Theta z\hat{k} \times \hat{r} \neq 0)$, but its integrated sum becomes equal to zero because of the inversion symmetry: (Figure 2a,b).

$$F^{\Psi}_{Wall} = G\int \hat{r}.\Psi\, dS \Rightarrow -1/2G \int \hat{r} \times (\nabla \times \vec{s})\, a\, d\theta dz = \Theta a \int_0^L z dz \int_0^{2\pi} \hat{t}\, d\theta = 0 \quad (6)$$

Therefore, the sum of the forces acting on the bar, whether they belong to the cross-sections or side walls, in the absence of body forces is identically equal to zero, which means that we can choose any point in the bar as an origin as shown in Figure 2a to calculate the torque terms [12].

We can choose the center of the constrained-bottom-end cross-section as a natural pivot point for the torque calculation, where the torsional displacements become zero. This choice is not completely arbitrary, but depends on the boundary

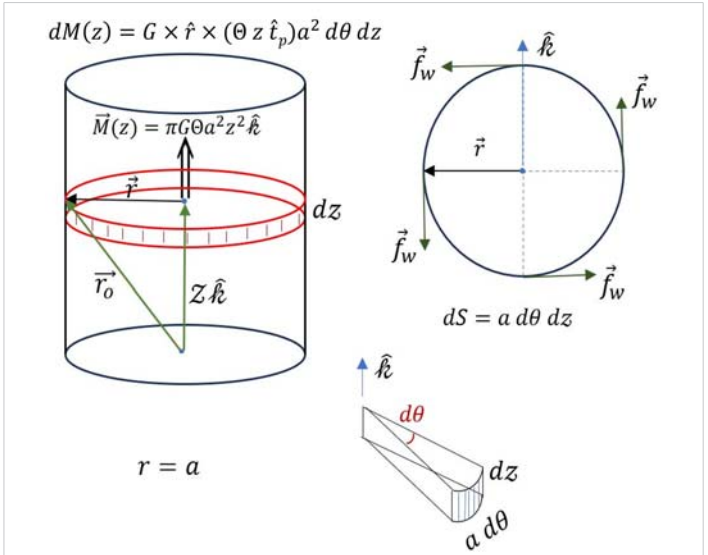

Figure 2: Shows the vectorial geometric connections employed in the computation of the global torque term $d\vec{M}(z) = G(\vec{r} + z\hat{k}) \times (\hat{k}.\Psi) dS$ associated with the force $\vec{f}_w = G(\hat{r}.\Psi)$ due to the anti-self-conjugate deformation tensor for side-wall surfaces. Shear modulus G is included in the torque $d\vec{M}$ ((z) formula.

conditions applied to the ends. If one chooses both ends to be free of surface traction forces and moments as counteracting sets, then one must choose the mid-plane of the bar or helical conformation as a natural reference system. Using Figure 1a,b the torque balance may be calculated in a similar manner in the absence of body forces as follows: Here, the position vector of the integration point is given with respect to the bottom clamp end of the bar (origin) (Figure 1a), and may be denoted by $\{\vec{r}_o = z\hat{k} + \vec{r}\}$ Then, the contributions to the torque; $M^{\Psi}_{End} = G\int(\vec{r} + z\,\hat{k}) \times \left(\hat{k}.\Psi\right) dA$ from the first $[z\,\hat{k}]$ and second terms are follows:

$$\int z\hat{k} \times \left(\hat{k}.\Psi\right) dA = -1/2G\int z\hat{k} \times \left(\Theta r\hat{t}\right) r dr d\theta = 1/6G\Theta z\, a^3 \int \hat{r} d\theta = 0$$

$$M^{\Psi}_{End} = G\int \vec{r} \times \left(\hat{k}.\Psi\right) dA = -1/2\, G\Theta \int \vec{r} \times \left(r\hat{t}\right) r dr d\vartheta$$

$$= 1/2G\Theta\bar{k}\int r^3 dr d\theta = \pi G\Theta a^4 \hat{k}/4 \qquad (7)$$

And

$$\int z\hat{k} \times \left(\hat{k}\ddot{O}\right) dA = -1/2G\int z\hat{k} \times \left(\dot{E}\, r\hat{t}\right) r dr d\grave{e} = 1/6\, G\grave{E}\, z\, a^3 \int \hat{r} d\grave{e} = 0$$

$$M^{\Phi}_{End} = G\int \vec{r} \times \left(\hat{k}.\Phi\right) dA = 1/2G\Theta \int \vec{r} \times \left(r\hat{t}\right) r dr d\theta$$

$$= 1/2G\Theta\hat{k}\int r^3 dr d = \pi\ G\Theta\int r^3 dr = \pi\ G\Theta a^4 \hat{k}/4 \qquad (8)$$

The total torque acting on the free end of the bar is the sum of the above findings: $M^{\Phi,\Psi}_{End} = \pi G\Theta a^4 \hat{k}/2$. This figure is exactly equal to the one was obtained by Landau and Lifshitz [5] for circular rod, and $\pi G a^4/2$ was by then called as ``the torsional rigidity,'' and where $J = \pi a^4/2$ is the polar moment of inertia of the section when the section is circular [11]. Similarly, the same result can be deduced from the formula obtained for the elliptical cross-section by Timoshenko and Goodies and Fung [2,11], $M_t = G\theta\pi a^3 b^3 \left(a^2 + b^2\right)$, using the stress function, which was first introduced by Prandtl [4].

These rigorously obtained results prove that the self- and anti-self- conjugate parts of the deformation tensors produce exactly the same torques for pure torsion applied to a circular bar, the summation of which is identical to that reported by Timoshenko and Goodier [4] and Landau and Lifshitz [5]. Including Saint-Venant [13,14], they all missed a very important contribution to the torque from the sidewall surfaces through the anti-self-conjugate part of the deformation tensor, which also reveals [Figure 2a,b] the importance of the nonvanishing shear force field $\Theta z\hat{t}$ acting on the sidewalls along the circumference tangent vector directions, $\hat{t}$. This creates an extra-integrated torque term, which is directed along the z-axis and has a magnitude that depends quadratically on the distance L^2 the cross-section away from the constrained bottom clamped end of the bar, as follows: [Figure 2a,b].

$$M^{\Psi}_{Wall}(z) = G\int \left(\vec{r} + z\,\hat{k}\right) \times \left(\hat{r}.\Psi\right) dS = G\int \left(\vec{r} + z\,\hat{k}\right) \times \left(\Theta z\,\hat{t}\right) dS,$$

And

$$M^{\Psi}_{Wall}(z) = G\int \left(\vec{r}\right) \times (\Theta z\,\hat{t}) a d\theta dz + G\int \left(z\,\hat{k}\right) \times \left(\Theta z\,\hat{t}\right) a d\theta dz, \qquad (9)$$

i) $G\int_0^{z,2\pi} \hat{r} \times \left(\Theta z\,\hat{t}\right) a^2 d\theta dz = \pi G\ \Theta a^2 z^2 \hat{k}$

ii) $G\int \left(z\,\hat{k}\right) \times (\Theta z\,\hat{t}) a d\theta dz = -1/3G\Theta a z^3 \int_0^{2\pi} \hat{r}\, d\theta \equiv 0$

$$M^{\Psi}_{Wall}(z) = 2\pi\Theta G a^2 \hat{k}\int_0^z z dz = \pi G\Theta a^2 z^2 \hat{k} \rightarrow M^{\Psi}_{Wall}(z) = \pi G\Theta a^2 L^2 \hat{k} \qquad (10)$$

Where L denotes the full height of the bar along the z-axis. This expression clearly shows that a new torque term is produced because of the circumferential shear forces $\left(\Theta z\,\hat{t}\right)$ acting on the cylindrical sidewall, which is directed parallel to the normal vector of the free-end surface of the bar, and the intensity of its action on the circumference of a given cross-section along the bar increases monotonically with the distance from the constrained bottom end of the bar. According to the statement made by Saint-Venant [1] and A. E. H. Love [15], which is also stated as `the principle of equivalence of statically equipollent systems of load' by Young [16]. This should be balanced by the externally applied torque $M^{\Psi}_{Wall}(L)$ at the free end, in addition to the other torque terms $M^{\Phi,\Psi}_{End}$ calculated above. The ratio of the torque terms $M^{\Psi}_{Wall}(L)/(M^{\Psi}_{End} + M^{\Phi}_{End}) = 2L^2/a^2 \gg 1$ is much greater than that calculated by those who neglect the circumferential shear stresses acting on the sidewall of the cylindrical bar. This extra torque term should be applied to the free end of the bar to maintain torsional deformation of the static equilibrium state of the bar. The authors working on the same torsion problem from the beginning chose to work with the strain tensor using a cylindrical coordinate system, where the compatibility requirements were put into the proper format by Lamb and Clapeyron [17].

Torque in helical conformation

All our findings, with the exception of the torque term associated with the side wall, can be immediately adapted for a simple helical bar with circular cross sections with the transformation of the three-pot vector set attached to the cross section of the bar $\{\hat{i}, \hat{j}, \hat{k}\}$ to the circular cross section of the helical conformation, making use of its geometric identity, $\{\hat{n}, \hat{b}, \hat{t}\}$. While we are doing this, we have a right-handed helix in our mind. Namely; $\hat{k} \Rightarrow \hat{t}$ that is the replacement of the surface normal of bar with the tangent vector of the helix, which is now becomes the surface normal of the circular cross section of the helical bar that is assumed to be doesn't show any warping. We can also define the plane of the circular cross-section of the helix as $\hat{t} = \hat{n} \times \hat{b}$, where $\hat{b} \Rightarrow \hat{j}$ is the binormal, and $\hat{n} \Rightarrow -\hat{i}$ is the principal normal vector of the helix, which forms the mid-meridian of the helical bar. The rate of change in the orientation of the binormal vector with respect to the arc length $d\hat{b}/d\ell - \lambda\hat{n}$ is called the torsion of the helix. where $\lambda \equiv \Theta$ is the torsion, which is an invariant quantity defined as $\lambda = (1/R)\sin\beta\cos\beta$ for the simple helix. Here, β is the angle between the generator of the circular cylinder and the tangent vector of the helix and is assumed to be constant. Similarly, the curvature κ is defined as $d\hat{t}/d\ell = \kappa\hat{n}$, which is the rate of change in the orientation of tangent vector $\hat{t}$ with respect to the arc

length $d\ell$; $d\omega/d\ell \Rightarrow \pm\kappa$, where the sign is arbitrarily assigned to the concave and convex surfaces. where $d\omega$ is the infinitesimal angular difference between two successive tangent vectors along arc length d. This is also an invariant quantity for a simple circular helix and is given by $\kappa = (1/R)\sin^2\beta$ [9].

It can be seen that the plane of the circular cross section of the helical conformation of the circular ring rotates around the surface normal, which is called the principal normal designated by vector $\hat{n}$. Target and binormal vectors vary concurrently along the curve because $\hat{n} = (\hat{b} \times \hat{t})$. After differentiating this vector connection, the following relationship is obtained: $d\hat{n} = d(\hat{b} \times \hat{t}) = d\hat{b} \times \hat{t} + \hat{b} \times d\hat{t} = (\lambda\hat{b} - \kappa\hat{t})d\ell$. The projection of $d\hat{n}$ over the binormal can be expressed as $d\hat{n} \cdot \hat{b}\hat{b} = \lambda\hat{b}d\ell$. The simultaneous actions of this infinitesimal projection vector in collaboration with the definition of $d\hat{b} = -\lambda\hat{n}d\ell$ on the $(\hat{t}, \hat{n}$ and $\hat{b})$ orthonormal axis set, respectively, results an infinitesimal clock wise rotation of the cross-section of helical conformation around the tangent vector $\hat{t}$, which may designated by $d\vec{\varphi} = \lambda\hat{t}d\ell \Rightarrow \vec{\Theta} = d\vec{\varphi}/d\ell = \lambda\hat{t}$. where the $\vec{\varphi}$ vector also describes the rate of twist of the oscillatory plane per unit arc length, the magnitude of which is given by $Mod\,\vec{\Theta} = \lambda$.

This presentation shows that for a helical conformation, one may take geometric torsion parameter λ of the simple helix as the ``torsion ``of the curve ``denoted by λ, and defined as the rate of rotation of the twist angle ϕ per unit length of the rod or ring. This means that two neighboring cross sections at distance d will rotate through a relative angle $d\varphi = \lambda d\ell$ [so that $\lambda = d\varphi/d\ell$]. For helical conformations, this means that the infinitesimal relative orientation difference $d\vec{\varphi}$ of two successive cross sections, separated by the infinitesimal arc length denoted by d may be designated by $d\vec{\varphi} = \lambda\hat{t}d$. where $\hat{t}$ is the unit tangent vector of the helix, which is also the surface normal vector of the cross-sections of the twisted ``circular ring sector'' employed by Timoshenko and Goodier in their monumental work [4]. The following expression also rigorously proves that the vector product operation by $\delta\vec{\varphi}$ on an arbitrary unit vector $\hat{r}$ at the cross-section of the ring creates an infinitesimal displacement, which is perpendicular to the direction of the position vector in that plane, and the rotation is clockwise.

$$\delta\vec{\varphi} \times \hat{r} \Rightarrow \lambda\hat{t}d\ell \times -\hat{n}\cos\theta + \hat{b}\sin\theta = \lambda d\ell - \hat{b}\cos\theta - \hat{n}\sin\theta. \quad (11)$$

where $\hat{r}$ is the unit vector in our formulation, and the parameter $d\varphi/d \rightarrow \equiv \lambda$ is used extensively, which is designated by a parameter Ω in the literature, called the torsion angle by Landau and Lifshitz [5], which is misleading. Rather, it should be called the rate of variation of the torsion angle φ with respect to length ℓ, which is perfectly correct. The total contributions from the screw and the self-conjugate parts of the deformation tensor, with the exception of the sidewalls, are oriented along the surface normal of the circular cross-section designated by the tangent vector for the simple helical conformation, and it becomes.

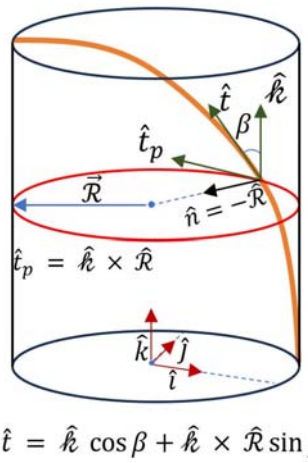

Figure 3: Decomposition of the side-wall torque of simple circular helix shown by red color line along the z-axis of the circular-cylindrical ring and the radial directions such as the principal normal $\hat{n}$, tangent of the local cross-section ^{t}p and $\hat{j}$, which is attached to the bottom clamp end of the ring.

$$M_{End}^{\Psi+\phi}(\ell) = M_{End}^{\Psi} + M_{End}^{\Phi} = \pi G\lambda a^4\hat{t}/2 \quad (12)$$

Figure 3 shows one way to decompose the tangent vector of helix $\hat{t}$ is to take its projection over the directions of $\hat{k}$ and $\hat{k} \times \hat{R}$ directions, such as $\hat{t} = \hat{k}\cos\beta + \hat{k} \times \hat{R}\sin\beta$. Where $\hat{R} = \hat{i}\cos\theta + \hat{j}\sin\theta$ is the unit radius vector of the helix in the circular cross sections projected at the basal plane, which is opposite in direction compared to the unit principal normal of the helix, $\hat{n} = -\hat{R}$. In Figure 3 $\{\hat{R},,\hat{t}p\hat{k}\}$ forms an orthonormal set of vectors, and the last two vectors defines a plane, which is tangent to the circular cylinder and holds the local generator as well as the tangent vector of the circular helix denoted by $\hat{t}$. Here, $\hat{k} \times \hat{R}\sin\beta$ = exp (- i θ) sinβ is the projection of the tangent vector of the helix over the tangent vector of the circular cross-section.

This vector is defined by the local radial direction with a π/2 degrees shift in the anticlockwise direction and $i = \sqrt{-1}$. The first term constitutes the projection of the torque along the fixed $\hat{k}$ direction, namely, the z-axis of the cylinder, and the second component may lie in the basal plane and is oriented perpendicular to the principal normal $\hat{n} = -\hat{R}$ of the helix. This clearly shows that the torque causes a precession motion following changes in the azimuthal angle θ along the helical backbone structure. Here, the apex angle is β = arcs $(\hat{t} \cdot \hat{k})$, and after that substitution, this expression in the torque equation $M_{End}^{\Psi+\Phi}(\ell)$, be written as the following set of relationships:

$$M_{End}^{\Psi+\phi}(\theta) = 1/2\pi G\lambda a^4\hat{t} = 1/2\,\pi G\lambda a^4\,\hat{k}\cos\beta + \hat{k} \times \hat{R}\sin\beta \quad (13)$$

And

$$M_{End}^{\Psi+\phi}(\theta) = 1/2\pi G\lambda a^4\hat{t} = 1/2\,\pi G\lambda a^4\,\hat{k}\cos\beta + \hat{t}p\sin\beta \vee \hat{k}.\hat{t}p = 0$$

Where $C = G\lambda\pi a^4/2$ is called the ``torsional rigidity'' by Landau and Lifshitz [5] for a circular cross section with a moment of inertia denoted as $I = \pi a^4/2$. Here, a is the radius of the circular ring model of the helix, which is about a few

fractions of an Angstroms for the alpha -peptide [3]. This torque contribution also depends on the azimuthal angle variations along the helix owing to $\hat{R}(\theta)$, where the tangent vector describes a rotation around the z-axis with a constant apex angle denoted as β. where $i=\sqrt{-1}$ is an imaginary unit number.

$$M_{End}^{\Psi+\phi}(\theta)=1/2\pi G\lambda a^4\begin{bmatrix}\&\cos\beta\hat{k}+\sin\beta\left(\hat{j}\cos\theta-\hat{i}\sin\theta\right)\\=\cos\beta\hat{k}+\sin\beta\exp(-i\theta)\\=\cos\beta\hat{k}+\sin\beta\hat{t}\,p)\end{bmatrix} \quad (14)$$

Here, $\hat{k}\times\hat{R}=\left(\hat{j}\cos\theta-\hat{i}\sin\theta\right)$ may be written in the complex space, which clearly shows the 90° anti-clockwise rotation of the $\hat{R}$ clearly, namely, $\hat{k}\times\hat{R}=\exp(-i\theta)=\hat{t}\,p$, where $\bar{R}$ is the radial position vector in the cylindrical coordinate system $\{z\hat{k},\bar{R},\theta\}$, and $(\hat{k}.\hat{R})=0$, $\hat{t}_p$ is the unit tangent vector of the circular cross-section, and normal to the $\hat{k}$ and $\hat{R}$ unit vectors. The last expression above clearly shows that the radial component of the torque is directed along the tangent vector $\hat{t}_p$ of the circular cross-section of the circular cylinder having an azimuthal angle of $\theta_r=\left(\theta+\frac{\pi}{2}\right)$, and its magnitude $\left|M_r^{\Psi+\Phi}\right|=1/2\pi G\lambda a^4\sin\beta$ is constant along the helix.

The right-handed rectangular coordinate system (i.e., anti-clockwise) is considered to attack the cross-section of the bottom end of the bar for the vector cross-product operations of $\{\hat{i},\hat{j},\hat{k}\}$. The sidewall formulation of the helical bar involved refinement of the adaptation procedure. Expressions such as $\int_0^L\hat{k}\,zdz$, which appear in the integration procedure of the sidewall torque, should be replaced by $\int_0^L\hat{t}\,d\ell$. Then, the torque associated with the sidewall may be written as $M_{Wall}^{\Psi}(\,)=2\pi G\lambda a^2\int_0\hat{t}\,d$ for the sidewalls of the circular cross-sections of the helix. One may rewrite in terms of vectorial properties of helical conformation given in reference [9], such as the unit tangent vector $\hat{t}$ in Cartesian coordinates using β inclination angle, which is constant, and the azimuthal angle θ, as follows: $\hat{t}=\cos\beta\hat{k}+\sin\beta\exp(-i\theta)$ which clearly show the rotation and precession motions. The length of helix and the azimuthal rotation angle θ are not independent variables and have the following relationship: R θ sin β, Similarly, for the pitch height p = cos $\beta$where R is the radius of the helix.

$$M_{Wall}^{\Psi}(\theta\ell)=2\pi G\lambda a^2\left\{1/2\hat{k}\ell^2\cos\beta+\sin\beta\int_0^{\ell}d\ell\exp(-i\theta)\right\}$$
$$=2\pi G\lambda a^2\left\{1/2\hat{k}\ell^2\cos\beta+R^2\,csec\beta\int_0^{\theta}\theta d\theta\,exp(-i\theta)\right\} \quad (15)$$

It is not obvious that the angular expression between brackets is a periodic function of 2, π even though the principal normal makes a full cycle when θ varies from zero to 2π. This is because the normalized amplitude of the precession motion, denoted by $R^2\csc\beta\,\theta$ increases monotonically with an increase in the azimuthal angle towards the free end. It takes the following value: $M_{Wall}^{\Psi}(L)$, for the global moment balance, and L is the total length of the helical conformation. Here, we use the following transformation of variables while maintaining the geometric description of a simple helix: $\ell=\theta R\csc\beta\Rightarrow d\ell=R\csc\beta\,d\theta$. where the first relationship connects the arc length of the helix with the azimuth angle θ in the cylindrical coordinate system, which varies from 0 to 2π for each full turn of the helical line around invariant axis $\hat{k}$. This gives the full arc length of the helix for n turns as $h_n=2\pi\mathbf{n}\,R\,\mathrm{csec}\beta$ and the full pitch height for n turns as $h_n=2\pi\mathbf{n}R\,\mathrm{ctan}\beta$. As (θ) is a periodic function of 2π, it can be expressed as (θ) = θ$R\csc\beta$. By substituting the decomposed form of the tangent vector of the helix into Eqs. (15), the following expression is obtained: Eq.(16) in terms of a three-pot orthonormal set of unit vectors $\{\hat{i},\hat{j},\hat{k}\}$ attached to the basal plane, before and after the integration procedure of the second term, we use the connections between the arc length and azimuthal angle for the helix obtained from the last expression for the torque term associated with the screw part of the deformation tensor.

$$M_{Wall}^{\Psi}(\ell,\theta)=\pi\lambda Ga^2\left\{\cos\beta\int_0\hat{k}\,d\ell+\sin\beta\int_0^{\ell}\ell d\ell\exp(-i\theta)\right\} \quad (16)$$
$$=\pi\lambda Ga^2\left\{1/2\,\hat{k}\cos\beta\ell^2+R^2\csc\beta\int_0^{\theta}\left(\hat{j}\cos\theta-\hat{i}\sin\theta\right)\theta d\theta\right\}$$

$$M_{Wall}^{\Psi}(\theta)=\pi\lambda Ga^2R^2\csc\beta\left\{1/2\,\hat{k}\,\theta^2\mathrm{ctan}\beta+\left\{\begin{matrix}\left(\hat{j}\cos\theta+\hat{j}\,\theta sin\theta\right)-\hat{j}\\\&\\+\left(\hat{i}\,\theta cos\theta-\hat{i}\sin\theta\right)\end{matrix}\right\}\right\} \quad (17)$$

In Figure 4 the radial component $R(\theta+\pi/2)\hat{k}\times M_{Wall}^{\Psi}(\theta)$ of the torque according to the formula given by the second term in Eq.(17), is plotted, which rotates around the z-axis of the helical conformation and draws a spiral path, while its azimuthal angle θ changes $0\le\theta\le\theta_T$ continuously along the helix. The precession angle of the torque ϑ may be obtained from the following expression. where one has; tan $\vartheta=R(\theta)/\hat{k}.\overline{M}_{Wall}^{\Psi}(\theta)$.

$$\vartheta=\mathrm{atan}\frac{2(\cos\theta-1+\theta\sin\theta)^2+(\theta\cos\theta-\sin\theta)^{21/2}}{\theta^2\mathrm{ctan}\beta} \quad (18)$$

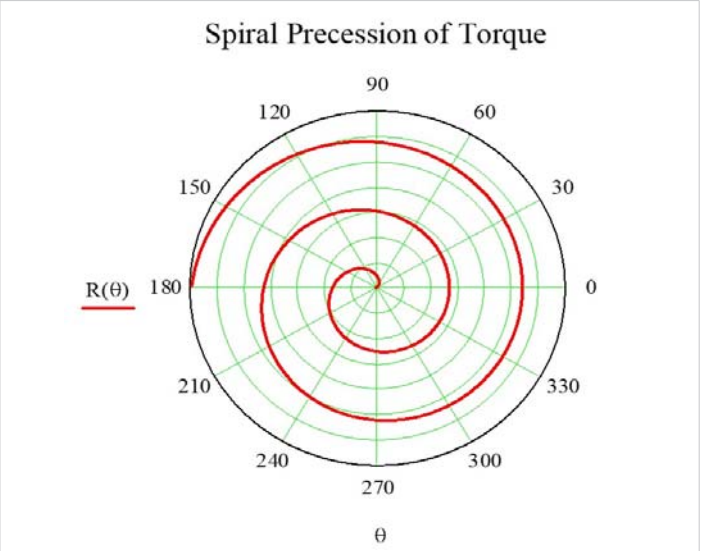

Figure 4: The radial component of the torque R(θ) according to the formula given by the second term in Eq. 17, rotates around the z-axis [$\hat{k}$] of helical conformation, and draws a spiral path while its azimuthal angle changing as 0 ≤ θ ≤ 6π continuously along the helix.

In Figure 5 the precession angle ϑ between the torque and z-axis obtained from screw symmetric part of the deformation tensor is plotted with respect to the azimuthal angle (θ/2π) for the first four full cycle around the z-axis of the helix for two different tangent inclination angles β (or two different pitch heights: $h1=2\pi R \times 173$, $h2=2R\times0.325$) namely β1=π/6 (red) and β2=72° (blue). This plot clearly shows that the precession angle of the torque initially starts with the inclination angle of the tangent of the helix with respect to the generators designated as β and then decreases continuously with the azimuthal angle θ.

Particularly during the first cycle, it shows a drastic decrease in the inclination angle, even though its projection on the basal plane increases almost linearly with some imposed periodic oscillations with a wavelength equal to 2π. At a multiple of 2π of the azimuthal angle, there are plateaus in the amplitude variations, which indicate that these are quasi-nonequilibrium stationary states for precession motion. After a few more cycles, the direction of the torque asymptotically approached the orientation of the z-axis, regardless of its initial direction.

This off-diagonal part of the torque has such variations in the direction that it tries not only to suppress the pitch height of the initial few cycles, but also applies a large twist moment on the first ring to perform a 180o °rotation around the principal normal $\hat{n}$. This effect increased as the initial inclination angle β increased (small pitch height). The oscillatory behavior of the amplitude variations can be seen clearly in Figure 6. (aqua), where the inclination angle of the torque and magnitude of the basal component are plotted using Eq. (16) with respect to the azimuthal angles by considering β= 30°(red) and 72°, (blue),

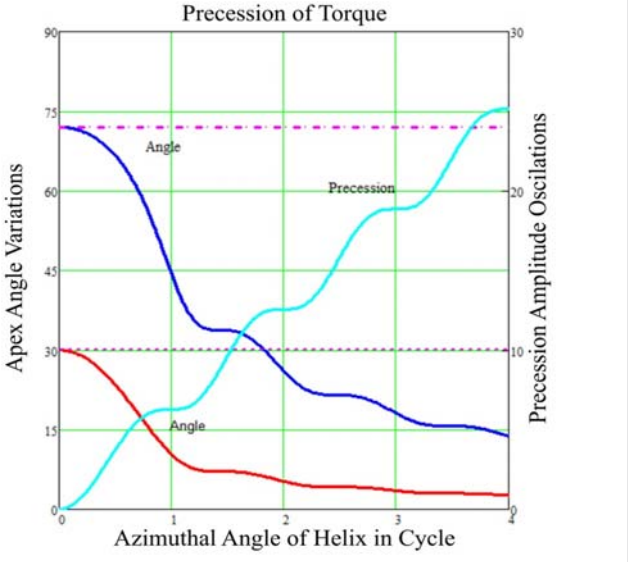

Figure 5: Cyclic precession motion of the torque ϕ is presented with respect to the azimuthal angle of helix as calculated from Eq. 18 (red and blue lines). The torque asymptotically adjusting itself parallel to the z-axis of helix, while apex angle decreasing to zero asymptotically. The precession amplitude also shows a periodic oscillation with an interval of 2π.

respectively. These are also invariant angles between the tangent vector and generators of the helix. Close inspection of the amplitude plot shows oscillations with a periodicity equal to 2π.

During the first cycle of precession motion of the torque, as described by Eq. (17), exerts a torsion moment over the oscillation plane through its off-diagonal component oriented along the principal normal of the helix, forcing it to rotate clockwise. This is an interesting finding that clearly shows the importance of the constrained end in stabilizing the torque. This could be used as a mimic in practice by placing rather heavy and/or highly rigid molecular cis-isomer constituents at the end of the steroid skeleton six-ring [18] chain to increase its local torsional moment on the A-ring side because of its additive character in the alignment with two other components of torque deduced directly from the self- and anti-self-conjugate part of the deformation tensor.

In Figure 6 the normalized projected torque oriented along the surface normal of the circular cross-sections using Eq. 17 are plotted, where $\pi\lambda Ga^2$ is employed as a normalization factor that arises from the sidewall shear stress fields of helical conformations. Variations in the apex angles were also plotted to demonstrate their behavior. Two different β apex angles were selected namely; 72° (blue) and 30° (red). An increase in the beta angle or pitch angle does not change the upper limit of the critical range, which is approximately 120° but enhances its effect by increasing the intensity of the temporal –twist moment on the oscillatory plane of the first ring and moves in both directions by applying the same right-hand twisting.

For a helical bar, the expression in Eq.17 can be also written in terms of the arc length instead of, θ which is also a function of the arc length:

$$M^{\Psi}_{Wall}(\theta\ell)=2\pi G\lambda a^2\left\{1/2\hat{k}^2\cos\beta+\sin\beta\int_0 d\ exp(-i\theta)\right\}$$

$$=2\pi G\lambda a^2\left\{1/2\hat{k}^2\cos\beta+R^2csec\beta\int_0\theta\, d(\theta)(\left(\hat{j}\cos\theta-\hat{i}\sin\theta\right))\right\}$$

$$M^{\Psi}_{Wall}(\ell)=\pi G\lambda a^2\left\{\hat{k}^2\cos\beta+2R-\left[\ell\hat{n}+R\,\mathrm{csec}\beta\hat{t}P-\hat{j}\,R\mathrm{csec}\,\beta\right]\right\} \quad (19)$$

As illustrated in Figure 6 , $\hat{t}p=\hat{k}\times\hat{R}=-\left(\hat{i}\sin\theta-\hat{j}\cos\theta\right)$ is the unit vector, which is the tangent of the circular cross-section of the helix and designates not only the direction of the precession motion of the torque term but also its amplitude dependence on β. $\hat{n}=-\hat{R}$ is the principal normal vector of the helix, which is directed towards the axis of the cylinder and is perpendicular to both tangents $\{\hat{t}_p,\hat{t}\}$ and binomial, denoted by $\hat{b}=-\hat{n}\times\hat{t}$. The first term in the above equation shows that the torque causes not only a simple rotation about the z-axis but also that its amplitude along the z-axis grows steadily with the quadratic function of length, while its precession amplitude increases linearly with the azimuthal angle. The latter motion follows a spiral path, as illustrated in Figure 4. where the genuine torsion associated with the helix is defined

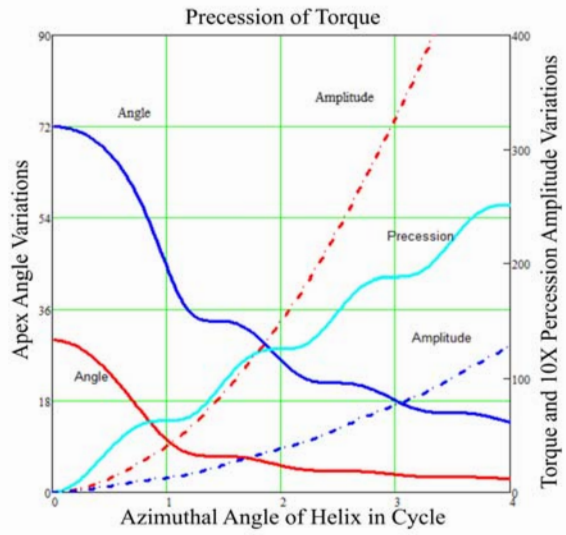

Figure 6: The apex angles β and precession amplitudes of torque are plotted for two different apex angles β = 30° (red) and 72° (blue). The projections of torque along the z-axis are given by red and blue dash-dots-lines, respectively. These show that the amplitude for the small angle grows much faster than the large one. The precession amplitude oscillations show periodic temporal stationary states at the integer n multiple values of 2π.

as $d\hat{b}/d\ell - \lambda\,\hat{n}$. Here, λ measures the arc length rate of turning of the binormal unit vector $\hat{b}$, similar to curvature κ, which is also a scalar quantity that measures the arc rate of the turning tangent vector $\hat{t}$.

The torsional torque of a bar with a circular cross section is an invariant quantity because the rate of torsion per unit length is constant along the bar. This means that it does not change from one end to another. However, the torsional displacement measured by the cumulative twist angle varies linearly along the bar, which is given by $\varphi_T = \theta = \ell\lambda$. One may write the following relationship, that can be obtained from Eqs. (7, 8) for the rate of change in the torsional torque of the helix by replacing the $\hat{k}$ vector with the tangent vector $\hat{t}$ of the helix, where $\hat{t}$ varies with the arc length or azimuth angle θ:

$$(M^{\Psi}_{End} + M^{\Phi}_{End}) = \frac{1}{2}\pi G\lambda a^4\hat{k} \Rightarrow \frac{1}{2}\pi G\lambda a^4\hat{t}(M^{\Psi}_{helix} + M^{\Phi}_{helix})$$

$$= \frac{1}{2}\pi G\lambda a^4\begin{bmatrix} \&\hat{k}\cos\beta + \hat{k}\times\hat{R}\sin\beta \\ \& \\ \&=\hat{k}\cos\beta + \hat{t}\,p\sin\beta \end{bmatrix} \quad (20)$$

Where the first term stays constant having directed along the z-axis of the helix, but the second term which makes rotation around the cylinder axis $\hat{k}$ by sweeping a perfect cycle having a radius equal to sinβ as can be seen from the explicit expression: $\hat{t}\,p = -k\wedge\hat{n} = -\left(\hat{i}\sin\theta - \hat{j}\cos\theta\right)$ dictates direction of the rotation of the principal normal denoted by $\hat{n} = -\hat{R}$ around the z-axis.

Pure bending adapted for circular helix

The pure bending and twisting of a circular ring sector have been extensively treated by Göhner [19] in various studies using the classical theory of elasticity. Later, his unabridged results were carried by others into their books, namely by Timoshenko and Goodies [2], who communicated with him by letters. Göhner approach to the problem of pure torsion as well as to the bending was to find a set of successive approximation for the stress functions, which were supposed to be satisfying not only Airy differential equation in 2D space deduced from the axially symmetrical stress distribution problems, [20] but also the compatibility requirements. Original set of equations were given in the cylindrical coordinate system, which were obtained by Lame' and Clapeyron [17] (1831) using the force equilibrium equation $\nabla\cdot\Omega + \rho\vec{F} = 0$, in the absence of the body force $\vec{F} = 0$. Where, Ω is the stress dyadic, which is assumed self-conjugate tensor, and then the strain tensor counterpart supposed to satisfy the compatibility connection given by ∇ × Φ × ∇=0. Therefore, from the beginning of his attempt to solve this problem by successive approximations, he completely lost the critical component of the torque originating from the non-vanishing circumference shear force field at the sidewalls, which was assumed to be zero or negligibly small to affect the results of the solution as a part of the boundary conditions. In fact, in the absence of the anti-self-conjugate part of the deformation, he would not have any change to discover the existence of the unusual term critical component. In fact, it is dangerous to start solving the elastic problems from the opposite direction, namely, setting a boundary value problem to find the stress and strain distribution functions relying on the ill-defined fact that the strain function would be unique if they satisfy the compatibility set. However, this satisfaction does not guarantee that anti self-conjugate part vanishes. Owing to the rotational character of the anti-self- conjugate dyadic (its divergence vanishes), it satisfies compatibility [10,11].

$$\nabla s = \Phi - 1/2I\times(\nabla\times s) \Rightarrow \nabla\times\Phi = -2^{-1}(\nabla\times(\nabla\times s)) \Rightarrow \nabla\times\Phi = -2^{-1}(\nabla\cdot s)\nabla - \nabla^2 s = -2^{-1}3\nabla \Rightarrow \nabla\times\Phi\times\nabla = -3/2\nabla\times\nabla \equiv 0. \quad (21)$$

Göhner argued that if two equal and opposite couples' M are applied at the ends of a circular ring center in the plane of the center line of the ring, they produce strain symmetrically with respect to the z-axis, and the shearing stresses $\tau_{r\theta}$ and $\tau_{\theta z}$ in the meridional cross-sections of the ring are zero. The remaining four stress components, $\{\sigma_r, \sigma_\theta, \sigma_z, \tau_{rz}\}$ must satisfy the equations of equilibrium for the case of symmetrical strain. The first approximation yields a solution, where all those three components $\{\sigma_r, \sigma_z, \tau_{rz}\} \Rightarrow 0$, out of four become zero with the exception of the uniaxial stress acting along longitudinal direction of the circular ring, as we denoted by unit vector $\hat{t}$; $\vec{\sigma}_\theta = -cEx\,\hat{t}$, where $c = 4M_b/\pi a^4 E$, E is the Young modulus of elasticity, and a is the radius of the circular cross section, X is distance of the point from the center, $I_{cm} = \pi a^4/4$ is the second moment of inertia with respect to the center of mass system (c. m.). Where by definition c is the rate of change in the orientation of tangent vector $\vec{t}$ with respect arc length, $c = d\alpha/d\ell \Rightarrow \kappa$. This is the definition of curvature, which may be designated as $\kappa = 1/R\sin^2\beta$ for a simple helix. Then one writes

$M_b = 1/4\,\pi a^4 E R^{-1}\sin^2\beta \Rightarrow \kappa EI$. Similarly, the Helmholtz free energy for a pure bending deformation, *m*.

The node of a simple helical conformation can be written as $F_B = 1/2\,M_b\kappa = 1/2EI\kappa^2 = 1/2\,E(\pi a^4/4)R^{-2}\sin^4\beta$ (erg/cm). A close inspection of beam vibration theory [11] shows that the SED for small deflections involves the term $\left(\partial^2 y/\partial x^2\right)^2$ in the integrand of $U = \int_0 EI\left(\partial^2 y/\partial x^2\right)^2 dx$, which is the square of the curvature of the 2D curve as a first-order approximation of $\kappa = \left|y^{'}\right|\left|\left(1+y^{'2}\right)^{3/2}\right|$. In fact, one can calculate the torque associated with the stress distribution by $M_\theta = \int_{-a}^{+a}\vec{\sigma}_\sigma \times \vec{r}dA$, and then write.

$$\begin{aligned}
&\vec{M}\theta(\theta) = -\kappa E\left]_{-a}^{+a}x\right.\begin{pmatrix}\&\,\hat{t}\times\vec{r}\ \text{or}\\ \&\,\hat{j}x-\hat{i}y\end{pmatrix}dA = +\kappa E\left(\pi a^4/4\right)\hat{j} = -\kappa E\left(\pi a^4/4\right)\hat{b}\Rightarrow\\
&\vec{M}\theta(\theta) = -\kappa E\left(\pi a^4/4\right)\hat{k}\sin\beta+\cos\beta\left(\hat{i}\sin\theta-\hat{j}\cos\theta\right)\Rightarrow\\
&\vec{M}\theta(\theta) = -\kappa E\left(\pi a^4/4\right)\left[\hat{k}\sin\beta+\cos\beta\exp\left(i\left(\frac{\pi}{2}-\theta\right)\right)\right]
\end{aligned} \tag{22}$$

In the last expression, we employed the complex notation for the rotation operation, where $\hat{j}$ axis is replaced by the imaginary axis denoted by $i = \sqrt{1}$. The expression in Eq. 22 shows that the direction of the torque designated by $\hat{j}$ corresponds $-\hat{b}$, which can be deduced from the following connection for the right-handed helix: $\hat{j} = -\hat{t}\times\hat{i} \Rightarrow -\hat{t}\times\hat{n} = -\hat{b}$. The second and third lines in Eq.22 shows that the bending torque causes a rotation around the z-axis of the helix with an apex angle given by $\omega = \text{atancotan}\beta = (\pi/2-\beta)$, which is 90° off the initial precession motion of the torque associated with the screw symmetric deformation tensor, as well as from the torsional torque terms acting on the free end.

Mechanical stability of helical conformations α-peptide

In the first part of this section, the electromechanical stability of the strained helical confirmations is treated under isothermal isochoric and isobaric conditions. A special reference for the application of this theory to the α-peptide structure of amino acid complexes is provided by employing two different irreversible thermodynamics methods according to the imposed constraints on the free variables to obtain a simple and manageable mathematical model. In our subsequent papers [21,22] on the spontaneous unfolding of helical conformations, we introduce a more general relaxation approach using the Lagrangian multiplier method to solve the extremum problem. While dealing with the electromechanical stability of this highly complex and discrete atomic skeleton of peptides, we are still insisting on remaining in the domain of the continuum approach. The most important outcome of the present naïve thermodynamic approach to the stability problem is the unique role of the interfacial Helmholtz free energy of the boundary layers enclosing and separating the peptide skeleton from its immediate internal and external aqueous solution environments, which may be characterized by a single electrochemical quantity, that is, the pH level [3]. As far as the critical or non-equilibrium stationary stable arc length of the alpha-helical conformation is concerned, for isochoric isothermal systems, there is only one physicochemical parameter that plays a major role, which is the ratio of the surface (interface) Helmholtz free energy and the shear modulus of elasticity, namely, f_s/G.

The precession apex angle of the torsional torque obtained from the skew part of the deformation tensor is initially equal to the inclination angle of the tangent of the helix but then continuously decreases with the azimuthal angle. The recession component of the unusual torque term, which is oriented parallel but opposite direction to the principal normal of the helix in the basal plane, it is the only component of the among the torsional torque terms may allow the incoming `A' ring to rotate around the principal normal of the helix to match the oscillation plane of the `B' unit for the easy formation of cis-fusion bonding. The strength of this component was minimal at the N-terminus of the first amino acid residue and then increased gradually. The strength of this component according to Eq. 17. and Figure 7. depend on csec β, implying that a smaller apex angle β is the intensity of the torque term.

The apex angle during the first cycle shows a factor of two reductions, which indicates that the effects of the constraint at the clamp end (N-terminal) of the helix are important for stabilizing the entire system. In addition to the torsional torques, the bending torque exists, which is aligned along the binormal axis of the helix, and has the capacity to turn not only the circular cross section but also the oscillatory plane, and then force the B ring to match the coming A ring to form a cis-fusion.

This point may be used as a mimic by placing heavy weight or stiff molecular side attachments similar to the N-edge to stabilize the initial steroid skeleton group, which also helps the incoming A ring to have the required 180o twisting to form cis-fusion with the B ring, as shown in Figure 7a. This twisting can be achieved by the temporal torsional torque spiraling around the z-axis of the helical conformation, which is represented by the second term in Eq. (17), which is as follows:

$$\begin{aligned}
&M_{Wall}^{\Psi,P} = 2\pi G\lambda a^2\left\{R-\hat{n}+R\,\text{csec}\beta\,\hat{t}P-\hat{j}\,R\text{csec}\,\beta\right\}\\
&M_{Wall}^{\Psi,Rad}(\theta) = -2\pi G\lambda a^2R^2csec\beta\left\{\left(\theta\hat{n}+\hat{J}\right)-\hat{t}P\right\}.
\end{aligned} \tag{23}$$

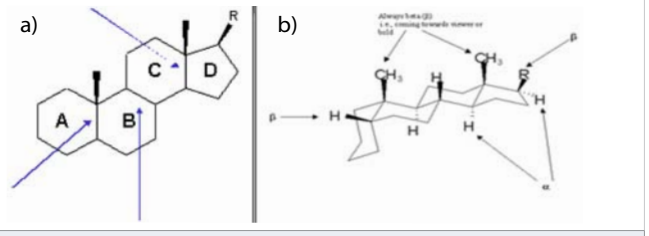

Figure 7: A typical Cis-Trans and Trans fusion sequence is demonstrated for β-Steroid skeleton structure. One needs 180° rotations of A-ring to be attached to the B-ring in order to form Cis-fusion bond. This is a very large twisting, which can only take place in nature either by the presence of highly localized thermal fluctuations or during the growth stage of the individual blocks.

This torque acts in a direction opposite to the principal normal $\hat{n}$, and forces the twist of the oscillation plane in the anti-clockwise direction for the right-handed helix. At the free end of helical conformations, where the torque terms arising from the torsion as well as from the bending should be balanced by the applied surface tractions and moments for the mechanical stability of the structure. However, in biochemical systems, such as folded peptides, it does not appear that their free edges sometimes experience any external moments by external agents for mechanical stability explicitly. It has been claimed that this task is accomplished at the C-ends of helical peptides by non-vanishing electrostatic counteracting forces. We show that this task can be accomplished spontaneously either by adjusting the surface Helmholtz free energy or by the presence of an excess pair of anti-align dipoles in the system under isochoric isothermal conditions.

It is also possible that without those edges being explode to external moments, the whole system might still be balanced mechanically either through the side-branching of residues, which connect the inner faces of the walls of the helical skeleton, or the whole system is in a viscoelastic state from the beginning and has very long relaxation times. In any case, the stored Helmholtz bulk free energy due to torsional deformation is given by the following expression, assuming that the system is isochoric and that all conceivable processes are isothermal:

$$\nabla F^{T}_{Mech}(\ell)=\int f_T dV=\frac{1}{2}G\int\begin{bmatrix}\nabla\vec{s}:\nabla\vec{s}=\\ 8\Theta^2 z^2+\\ 2\Theta^2\left(x^2+y^2\right)\end{bmatrix}dV$$

$$=G\Theta^2\left\{\pi a^4\ell/2+4\pi a^2\ell^3/3\right\}(\text{erg}) \quad (24)$$

It should be noted that only the minor $\begin{bmatrix}0 & 2\Theta z\\ -2\Theta z & 0\end{bmatrix}$ in the skew part of the deformation tensor contribute to the stored Helmholtz free energy in the bulk, which is given by $\frac{1}{2}G\int dV\left\{8\Theta^2 z^2\right\}\Rightarrow\{G\Theta^2 4\pi a^2\ell^3/3\}$. The other off-diagonal terms in the deformation tensor after the double inner product operation may be summed as $2\Theta^2\left(x^2+y^2\right)=2\Theta^2 r^2$, which involves the moment of inertia with respect to c.m. and the first term in Eq. (24). This may be neglected because it is a few orders of magnitude smaller than the contribution of the second term to torsional energy in a nanoscale environment.

Irreversible thermokinetics of helical conformation

Global Helmholtz free energy also involves a surface Helmholtz free energy that may be given by for the circular cross section helical form: $\nabla F^{T}_{S}(\ell)2\pi a\int f_S d=2\pi a f_S\ \ell$. Where f_s is the specific Helmholtz surface free energy, which should be replaced by the interfacial energy if the system in the interactive environments such as the aqua electrolytic solutions. In general, this quantity is positive in the absence of electrostatic and magnetic fields. However, in the case of deformed solids under isochoric conditions, the whole body is in a non-equilibrium state because of the existence of the stored residual elastic strain energy density in the bulk region as well as at the surface layer. The contribution of the surface or interfacial Helmholtz free energy to the global Helmholtz free energy appears to be a negative quantity that assists stability or avoids unfolding or fragmentation. This is due to the fact that any enlargement of the surface area regardless of its cause while keeping the volume invariant, produces substantial decrease in the elastic stored free energy [6-8] (strain recovery process) of the body under the isochoric and isothermal conditions. This in turn causes a decrease in the global Helmholtz free energy of the system, which means that it is a spontaneous natural change that pushes the system towards a non-equilibrium stationary state [6]. That hypothesis may be also justified by the Planck (1887) criterion [23] for isochoric isothermal changes for the closed system, which may be then connected to the Prigogine's positive definite internal entropy production hypothesis as a special case: $\delta\nabla S_{In}=-\mathrm{T}^{-1}\delta\nabla F_G\geq 0\ \forall\ \delta\mathrm{V}=0$, where equal sign for reversible (equilibrium) processes, and positive sign for the irreversible or natural processes. Namely:

$$\delta\nabla F_G(\ell)=\delta\nabla F_B(\ell)-\delta\nabla F_S(\ell)\leq 0$$

And

$$\nabla F_B\left(\ell\right)=\nabla F_{Chem}\left(V\right)+\nabla F_{Mech}\left(\ell\right)\forall\ \delta\nabla F_{Chem}(V)=0 \quad (25)$$

Which may be put into the following format for the present case, where the first term represents the bulk term that involves not only the chemical part $\nabla F_{Chem}(V)$ but also the elastic stored deformation energy $\nabla F_{Mech}(\ell)$ due to torque terms associated with pure torsion and bending. Because there are no composition or volumetric variations for the present stability problem, the bulk term involves only mechanically stored energy. The second term is the change in the surface Helmholtz free energy due to the change in the surface area of the helical conformations:

$$\begin{aligned}&\delta S_{Int}/\delta t=-1/T\delta\nabla F_G/\delta t\geq 0,\\ &\delta\ell/\delta t=-\mu/kT\left(3A\ell^2-B\right),\end{aligned} \quad (26)$$

The global Helmholtz free energy $\nabla F_G=\nabla F^{T}_{E}(\ell)-\nabla F_S(\ell)\Rightarrow A^3-B$ optimization with respect to the length displacements yields the following relationships: $\ell^*=(B/3A)^{1/2}$ cm, and where $\nabla F^*_G=-2/3\,\mathrm{B}(B/3A)^{1/2}$ erg/cm, which corresponds to, respectively, the critical length and the binding Helmholtz free energy of the helical conformation at the absolute stable state. The system parameters used in the above connections are A= $4\pi/3G\lambda^2a^2$ (dyne/cm^2) and B = $2\pi af_s$ (erg/cm). By using the following fundamental relationship, which is valid for the isochoric isothermal changes in closed systems: $\delta\nabla S^{G}_{Int}/\delta t=-1/T\delta\nabla F_G/\delta t$ between the rates of internal entropy production and the global Helmholtz free energy changes, respectively, one may obtain a very useful thermo-

kinetics expression: [24] $\delta\nabla S^{G}_{Int}/\delta t=-1/T\left(3A\ell^{2}-B\right)\delta \quad \delta t\geq 0$. The connection between the rate change in the Global Helmholtz free energy and internal entropy production was further elaborated by Ogurtani [23] for the irreversible thermodynamic formulation of quantum dot evolution kinetics in strained solid thin films under isochoric conditions. This expression may be decomposed according to Onsager's receipt, even though it would not be unique, into conjugate fluxes and forces to obtain a kinematic rate equation for the stability of the length of the helical conformation: $d\ell/dt=-\mu/kT\left(3A\ell^{2}-B\right)$, and by substituting the system parameter in their proper places, $d\ell/dt=-\mu/kT\left(G\lambda^{2}4\pi a^{2}\right)\left(\ell^{2}{}^{2}-\ell^{*2}\right)$. This kinetic equation may be integrated under two different initial conditions, namely, above and below the stationary state configuration, that is, $\ell=\ell_{R}>\ell^{*}$ and $\ell=\ell_{L}<\ell^{*}$. The analytical results of the integration are given for the following two domains [25]:

$$\frac{\ell-\ell^{*}}{\left(\ell+\ell^{*}\right)}=\frac{\ell_{R}-\ell^{*}}{\left(\ell_{R}+\ell^{*}\right)}\exp\left[-2\mu/kT\left(G\lambda^{2}4\pi a^{2}\ell^{*}\right)t\right]\forall\,\ell\geq\ell^{*} \qquad (27)$$

And

$$\frac{\left(\ell^{*}-\ell\right)}{\ell^{*}+\ell}=\frac{\left(\ell^{*}-\ell_{L}\right)}{\ell^{*}+\ell_{L}}\exp\left[-2\mu/kT\left(G\lambda^{2}4\pi a^{2}\ell^{*}\right)t\right]\forall\,\ell\leq\ell^{*} \qquad (28)$$

Inspection of the above set of equations shows that in both cases, the length of the helical conformation approaches asymptotically to the critical length, from top and bottom, respectively; $t\to\infty\Rightarrow\ell_{R}=\ell\searrow\ell^{*}$ and $\ell_{L}=\ell\nearrow\ell^{*}$. Using the above set of mathematical connections in Figure 8. two plots are produced that describe how the irreversible processes associated with these two non-equilibrium initial configurations of interest proceed asymptotically.

The third line in Eq. (26) designates Onsager's relationship between fluxes and conjugated forces. Where μ/kT looks very similar to the Einstein mobility, and this connection shows that when the length of helical conformation is less than the critical length (slope of Global Helmholtz free energy (GHFE) plot becomes negative) and then the natural isothermal process takes place, and the length starts to increase towards the minima in GHFE curve, which is nothing but the non-equilibrium stationary state according to the definition of Prigogine [26,27].

If there is some overshooting due to large fluctuations, then the opposite process takes over, which attempts to reduce the length of the helix until it reaches the critical length. This shows that this system, from the classical thermodynamics point of view, has an absolute stable state, as designated by the minima in the Global Helmholtz free energy plot. To illustrate the behavior of the isochoric system, we chose the following system tentative parameters: $f_{s}\Rightarrow B=15$ and A=15 to obtain real numbers for the graphical solutions shown in Figure 9a.

This again shows the stability of the peptide helical conformation even when β is very close to 82° which means

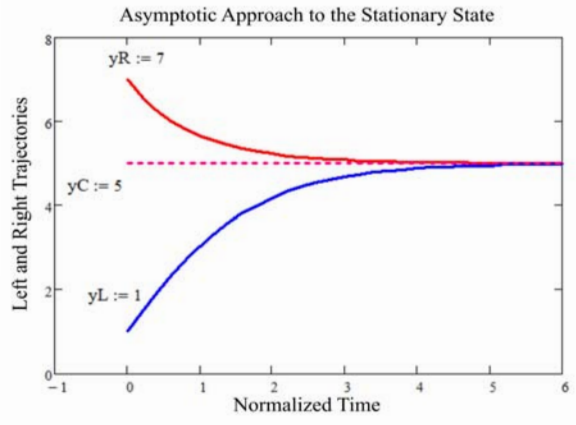

Figure 8: The asymptotic approaches from the left $\ell_{L}=7$ and right $\ell_{R}=1$ sides towards the stationary state configuration are illustrated by using scaled time t/τ and positions $\ell^{*}=5$ in connection with Eqs. (27,28) 25 . Where the inverse relaxation time is given by: $\tau^{-1}=2\ell^{*}\mu/kT\left(G\lambda^{2}4\pi a^{2}\right)$

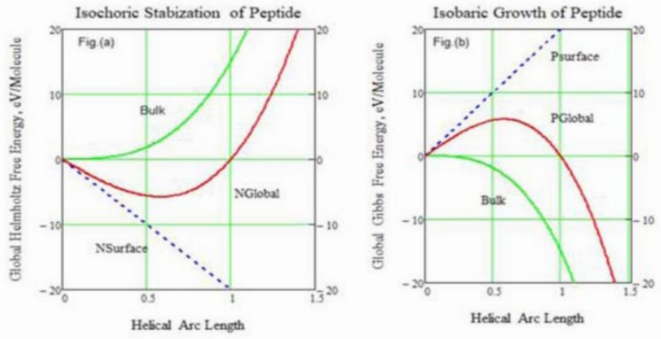

Figure 9: For the illustration the Global Helmholtz (red) and Gibbs (red) free energies for the isochoric Figure 9a and isobaric Figure 9b of helical conformation, the fictitious values of negative and positive surface free energies are employed, respectively. A = 15 and B= ±15. The calculated critical nucleation arc lengths and the extremum values of the Helmholtz and Gibbs free energy barriers are, respectively, found to be $\tilde{f}_{r}=G\left(\hat{k}.(\Phi+\Psi\right)$ ℓ^{*}= 0.59,0.56 and $\nabla F^{*}_{G}=-5.769$ *and* $\nabla G^{*}_{G}=+5.772$.

that the usual bending torque becomes very close to the maximum while the usual torsional torque term approaches zero; however, the main stability comes from the unusual torsional torque term formulated rigorously in this study, as demonstrated in Figure 9ab.

For isobaric Figure 9b and isothermal system, we have the following expression for the Global variation of the Gibbs Free energy with respect to arc length of a helical conformation: $\nabla G_{G}=-A\ell^{3}+B\Rightarrow\delta\nabla G_{G}=\left(-3A\ell^{2}+B\right)\delta\ell\leq 0$, where A=15 and $g_{s}\Rightarrow B=15$ is selected to produce the graphical solution of the problem, which is presented in Figure 9b. The following connections were obtained for the critical length ℓ^{*} of the helical nucleus and the activation energy barrier ∇G^{*}_{G} for the growth of the helix under constant traction (torques) and bending moments.

$$\ell^{*}=(B/3A)^{1/2}\text{ and }\nabla G^{*}_{G}=+2/3\,\mathrm{B}(B/3A)^{1/2}.$$

$$\nabla G_{G}=-A\ell^{3}+B\ell\Rightarrow\delta\nabla G_{G}=\left(-3A\ell^{2}+B\right)\delta\ell\leq 0$$

$\delta S_{Int}/\delta t=-1/T\delta\nabla G_{G}/\delta t\geq 0$, Positive Internal Entropy Production (29)

$$\delta\ell/\delta t = -\mu/kT\left(-3A\ell^2 + B\right),$$

The fourth equation in the above set was obtained by using the spilling technique of the internal entropy production inequality into conjugate forces and fluxes. Although this procedure is not unique, it satisfies the invariant transformation properties of conjugate forces and fluxes, as mentioned by De Groot [25]. The dynamic equation indicates that the direction of the change in the length $\delta\ell/\delta t < 0$ of the helical conformation is towards small sizes when the slope of the global Gibbs free energy (GGFE) curve is positive; otherwise, it is directed towards the growth domain, which is on the right side of the GGFE peak.

Where one could also introduce the contribution due to the Helmholtz free energy due to the pure bending associated with the helix, which is calculated in the previous section; namely: $\nabla F_M^B(\ell)1/2\,\ell M_b\kappa = 1/2\ell\,\kappa^2\left(E\pi a^4/4\right)$, where ℓ is the arc length of Helical conformation. Then the total bulk Helmholtz free energy associated with a helical conformation having circular cross section may be expressible by the following formula using our findings in this paper: Where, we have the following definitions for the system parameters designated above; $A = (4\pi/3)G\lambda^2a^2$ and $B = \left(2\pi af_s + \pi/2\left(2G\lambda^2 + E\kappa^2\right)a^4\right) \cong 2\pi af_s$.

Then one has;

$$\nabla F_{Mech}^B(\ell) + \nabla F_{Mech}^T(\ell)1/2\left\{E\kappa^2 + 2G\lambda^2\right\}\left(\frac{\pi a^4}{4}\right) + G\lambda^2\ell^3\left\{\frac{4\pi a^2}{3}\right\} \quad (30)$$

In the footnote calculations[a], which are given in , the shear modulus [28] is assumed to be G=1.0x10^{10} dyne/cm^2 (1GPa), which is estimated from the well-known relationships $\{E = \mathbf{v}^2 \times \rho$, and $G = E/2(1+\nu)\}$, where the mean values of the ultrasonic longitudinal propagation velocity, volumetric density, and Poisson's ratio, respectively, are given by v = 1.5 x 10^5 cm/sec., ρ = 0.92 gm/cm^3, and ν = 0.4 from measurements of L-alanine amino acid residues performed by Kumar [2] in an alcohol-water co-solvent at room temperature. The surface Helmholtz free energy is assumed to be approximately fs = 800 erg/cm^2 by observing the close connection between the unfolding total energy of the α-helix (L = 10 nm) and the pH (3-8) level of the water-alcohol solution data obtained experimentally by Idiris, et al. [3] (Ref-20, Figures 5,6.). The unfolding energy is reported to be approximately 20 eV/molecule or 2000 kJ/mole for the fully stretched conformation of (Glu)n -Cys at a pH of 8 at room temperature, assuming that the length is 10 nm. This experimentally obtained energy figure is one order of magnitude larger than the average effective energy of hydrogen bonds, $\langle E\rangle = -45$Kcal/mole (1.95 eV/molecule) for alpha-helix submerged in water, in the absence of π-helical hydrogen bonds, as reported by Hiltpold, et al. [29], which relies on extensive molecular dynamics studies. Here, the unusual torque terms, which is found to be $\nabla F_{\text{Mech}}^T = +7.71$ eV/molecule, where the critical arc length appears to be 98.7 A, while the binding Helmholtz free energy becomes -15.5 eV/molecule[b].

The best matching positions of the calculated stored elastic energy and global Helmholtz free energy values are marked by the blue solid circle and red diamond tip, respectively, on the free energy plots in Figure 10. the stability of the helical conformation can be explained quantitatively if one takes the surface Helmholtz free energy term [30] as fs=800 erg/cm^2, and the shear modulus G = 1GPa in this study. Those quantities produce the following numerics at the non-equilibrium stationary state; namely: the surface free energy as $\nabla F_S = -23.25$ eV/molecule, which is factor of two greater than the contribution coming from the stored elastic energy of 7.71 eV/mol due to unusual torque term in the global Helmholtz free energy. These large energy values come from the selected high G and fs values, but in reality, their experimental observations are closely related to the very ow pH 3-4 levels of the test environment and their drastic effects on the interfacial free energy through polar and/or nonpolar hydrophobic interactions [3].

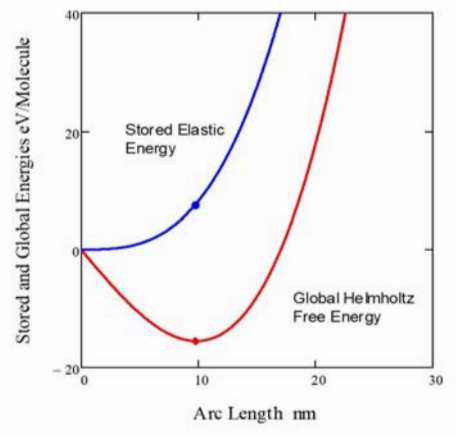

Figure 10: For the illustration, the Global Helmholtz Free energy (red) and the Stored Elastic energy (blue) due to unusual torque tem for the isochoric helical conformation. The calculated critical arc length and the binding Helmholtz free.

[a] If one uses, fs=800 erg/cm^2, G=1.0×10^{10} dyne/cm^2, λ= 2.34×10^6 cm^{-1}, and 2a=1.5 A, then one obtains: A=1.29×10^7 erg/cm, and B=3.77×10^{-5} erg/cm. Then, one finds a critical length of $\ell^* \cong 98.7$A from $\ell^* = (B/3A)^{1/2}$, and the critical Helmholtz binding free energy = -2.48x10^{-11}erg (-15.5 eV) for the non-equilibrium stationary state from=-2/3B (B/3A)$^{1/2}$. This amounts to 1.409 eV per amino-acid residue, which should be shared by its four main constituent atomic species {N, C$_\alpha$, C, O} that results - 8.139 Kcal/mole (0.352 eV/atom) for the helical α-peptide (3.6_{11} conformation, which is in excellent agreement with Ackbarow[36]. Who obtained, respectively, 11.1(9.9) and 4.87(3.08) Kcal/mole from the slow and fast dynamic tests. One order of magnitude decreases in G value while keeping the fs/G ratio invariant results a factor of ten reductions in all energetic values without changing the critical length.

[b] Reported values of the pitch high and diameter of α-helix are, respectively, 5.4A and 2R=12A in the literature. [29] Those may be used to calculate the inclination angle as β=81.84°, and the total length of helix 116A, and the arc length of a single ring as 38.06 A, respectively. The diameter of a residue is given by 2a=1.5 A. These data give us Torsion parameter as equal to λ=1/2R× sin (2β)≈ 2.34× 10^6 cm^{-1}. Amino acid residue length is 10.55A, and the mean distance between {C' and C'} or equally well {N by N} species is about 3.5 A. energy are, respectively, found to be $\ell^* \cong 98.7$A and $\nabla F_G^* = -15.5eV$ / molecule Blue solid circle and red diamond tip marks on the above energy profiles are calculated using the hypothetical data: fs=800 erg/cm^{2}and G=1GPa.

We have also tried to consider an extra term associated with the permanent electric dipole-dipole interactions, which prevail in most peptide conformations and are claimed to be the main structural stability agents without producing any substantial proof in the literature [28]. The dipole-dipole term is an intrinsic term, which should appear as an additive term in all characteristic functions, such as thermodynamic energy, enthalpy Helmholtz, and Gibbs free energies, but with sign reversal in the case of Enthalpy and Gibbs free energy [31], then one writes.

$$\nabla F_G = A^3 - B - C \Rightarrow \delta \nabla F_G = \left(3A^2 - B - C\right)\delta \le 0 \Rightarrow \ell^* = (B+C)/3A^{1/2}; \nabla F_G^* = -2/3\,(B+C)(B+C)/3A^{1/2} \quad \text{(Extremum)} \quad (31)$$

$$\nabla G_G = -A^3 + B + C \Rightarrow \delta \nabla G_G = \left(-3A^2 + B + C\right)\delta \le 0 \Rightarrow \ell^* = (B+C)/3A^{1/2}; \nabla G_G^* = +2/3\,(B+C)(B+C)/3A^{1/2} \quad \text{(Extremum)} \quad (32)$$

By considering C=5 (the proper ± signs are introduced in Eqs (31,32) for isochoric and isobaric systems, we obtained the following mappings: In particular, the isochoric solution produced very interesting results that showed stabilization of the helical conformation at the finite critical length.

This is a very important result to explain the strange behavior of peptides in practice, such as folding and unfolding, multiplications, or partition after having some critical size into two halves. Here, we demonstrate that the enhancement in the stability may be achieved by the D*D interaction because it produces an effect that implicitly reduces the surface specific free energies in both cases, namely, for the isochoric and isobaric isothermal changes, as shown in Figure 11a,b.

The potential energy of the dipole- dipole interaction between two permanent electrostatic dipole vectors separated from each other by $\vec{r}$ may be given by the following expression, where only the second term is used because of the on-plane positions of the residues $\vec{d}\cdot\vec{r} = 0$.

$$V_{d'-d} = -\vec{d}'.\left(\nabla\nabla\frac{1}{r}\right).\vec{d} = -\vec{d}'\,\frac{3}{r^5}\vec{r}\vec{r} - \frac{1}{r^3}I\vec{d} \Rightarrow +\frac{\vec{d}'.\vec{d}}{r^3} \quad (33)$$

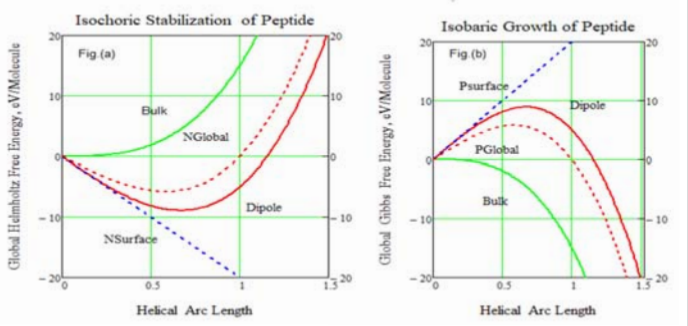

Figure 11: Stabilization of the helical conformation by the anti-align ↑↓ dipole-dipole interactions for the isochoric and isobaric systems is presented by using the following fictitious values: C = 5 (red -line) with d-d and C = 0 (red- dots) without d-d interactions, A = 15 and B = 15. Both systems show enhancements in their stabilization by lowering the minima in Isochoric system, Figure 11a and elevating the activation free energy barrier in the case of Isobaric systems, Figure 11b, and meanwhile the critical lengths show slight increase in both cases.

And

$$V_{d'-d} = -\frac{d_1.d_2}{4\pi\epsilon_o r_{12}}3\cos\theta_1\cos\theta_2 - \cos\theta_{12} \quad (34)$$

We may also employ the angular equation given above to account for misaligned dipoles. Where θ_{12} is the angle between the two oppositely charged dipoles and r_{12} is the distance between is the distance between the two molecules. θ_1 and θ_2 are the angles formed by the two dipoles with respect to the line connecting their centers. Aligned pairs with positive and anti-aligned pairs have negative potential energies. It is also important to determine the potential energy of the dipole moments of more than two interacting molecules. An important concept to keep in mind when dealing with multiple charged molecules interacting is that like charges repel and opposite charges attract each other. Therefore, for a system in which three charged molecules (two positively charged molecules and one negatively charged molecule) interact, the angle between the attractive and repellant forces must be considered.

In the present special case presented in Figure 12a,b. systematically, the mutual configurations of these pairs in the peptide blocks are such that their interaction may be represented by the last term in the above formula, because in most cases, dipole moments occur in pair-wise acting on *the same oscillatory planes* [32], either parallel or anti-parallel orientations.

These pairing arrangements automatically eliminate the first term and result in either negative or positive finite contributions, and $E_{d-d}(\pm) = \begin{pmatrix} +\rho(\uparrow\uparrow) \\ -\rho(\uparrow\downarrow) \end{pmatrix}\frac{1}{r^3}\vec{d}^2$ to the global Helmholtz and Gibbs free energies of the system, respectively. Where $\rho(\uparrow\uparrow)$ and $\rho(\uparrow\downarrow)$ are the volumetric dipole densities [#/cm^3] of the parallel and antiparallel dipole pairs in the helical conformation, respectively. Here, we do not agree with the argument of HoI [33] that three is the total cancelation of dipoles owing to the aggregate effect, except for the N- and C-termini, which have opposite electrostatic charges. HoI continues to argue that since the axis shift or pitch for each amino acid residue in the α-helix is 1.5 A, all dipoles cancel out except for the C- and N-termini. This argument, which may not be justified even for the stationary state configuration, when it

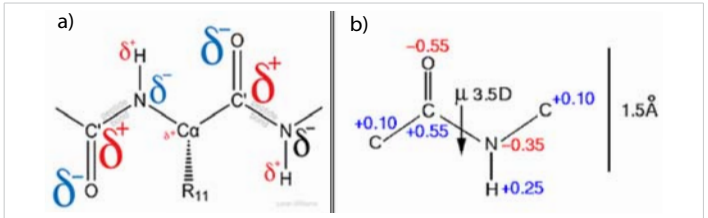

Figure 12: Electric Dipole distributions in amino acid blocks with anti-align and without align dipole pairs in Figure 12a. Where, there is only one strong anti-align pair out form by {C'-O and C'-O} in addition to the two align off-set pairs. In Figure12b, there is one align-pair, which is not assigned properly [33].

comes to the transition stage, would be completely collapsed, since the α-helix starts to relax towards unfolding because it is only a spontaneous decrease in the specific surface Helmholtz free energy density that can be achieved for the isochoric system. This change in the specific surface energy arises from the short-range electrostatic interaction between the highly monopolar surface characteristic of the amino acid backbone structure and its immediate hydrophobic environment, which helps reduce the interfacial surface free energy. This means that variations in the pH level of the aqueous solution, which is capping the alpha helix, may trigger pitch extension because of the back stresses originating from the stored torsional work injected during the folding stage. That pitch enhancement is accompanied by the simultaneous increase in the height of cylindrical cage of the helical conformation to reduce the residual torsional deformation characterized by $\lambda \Longmapsto 0$. Eventually, the result is complete unfolding toward the zero-inclination angle β or torsion $\lambda=1/R \sin\beta \cos\beta$, as has been observed recently in our simulation studies.

In practice, we have enough information about their arrangements and densities in particular peptide building blocks that we can make reasonable estimate about the excess density of the majority dipole pairs $\langle \pm\rho \rangle$ and their parity configurations, and use them in the calculation of the interaction potential; where `a' is the radius of helical circular conformation; namely: $E_{d-d}(\ell)=\langle \pm\rho \rangle \vec{d}^{\,2} / 4\pi\varepsilon_o r^3 \pi a^2 \ell \Rightarrow C\ell$. The negative and positive signs correspond to the anti-align and on-align pairs, respectively. There is a sign reversal in the C parameter when it is added to the Gibbs free energy, but not for the isochoric system. Therefore, we prefer to have an excess number of anti-align pairs, which go with a negative sign to Helmholtz free energy assists the surface free energy in stabilizing the structure for isothermal isochoric growth.

The calculations presented in the footnote[C] show that if one takes the shear modulus as G=109 dyne/cm, then two anti-align dipole pairs would be sufficient to stabilize the whole α-helix conformation with a critical binding energy of approximately 4 kcal/mol per amino acid residue, which is a factor of four higher than the measured unfolding energy of 11.1 (9.11) kcal/mol by Ackbarow, et al. [34] from the slow deformation test (SDT) performed on HB bonds in the α-helix. The Bell model [35] was used to analyze the dynamic force extension data obtained at various strain rates, which appears to be rather crude and unrealistic. The bond breaking energy of HB in water ranges typically 3-6 kcal/mole [36], which means that only three bonds are broken (SDT). On the other hand, there are approximately 11-13 HB bonds in the α-helix, which means that the total expectation value for the unfolding or binding free energy should be in the range of 33-80 Kcal/mole (1.43-3.5 eV/molecule). This unfolding energy range was also included in the energy landscape studies by Idiris, et al. [3] on (Glu)n Cys chains under different pH conditions (3.0-8.0 pH) using various extension rates and found a range of 2000-9000 kJ/mole (20-90 eV/molecule), which shows a monotonously decreasing convex connection between the total unfolding energy and pH level of the aqueous solvent solution.

Variational formulation of isochoric isothermal stabilty of helical conformation

Here, we clearly have a non-equilibrium deformation problem, such that the system, even in the absence of external tractions and body forces (with the exception of gravity), maintains its external form and internal integrity for a sufficiently long time. As shown in the main text, the most active and intensive component of this stored strain energy is the unusual torque term.

Keeping all these complications in mind, as a first step in handling this dynamic problem, we employ a quasi-static approach using a simple optimization procedure in connection with the planck criterion, which relies on the variational method [37]. Where, the Lagrange multiplier technique is utilized to address the constant volume constraint imposed on the problem while keeping the length and diameter of the amino acid backbone structure as free or independent variables. We could also enlarge our extremum problem such that the height (total pitch height) and radius of the hypothetical cylindrical shell or cage, which maintains the helical conformation of the amino acid chain backbone structure, can be adjusted while maintaining its volume and shell thickness. These constrained variations in the dimensions of the cage produce alterations in the inclination angle β of the helical conformation, which is reflected by the rotation λ and curvature κ associated with the amino acid skeleton[d] [21]. These ``frozen state' ' constraints on the cage will be lifted in our future work while dealing with the energetics of unfolding. The global Helmholtz free extremum problem can be represented by the following set. Here, a

$$\delta\nabla F(a\ell)\delta\left\{\frac{4\pi}{3}G\lambda^2 a^2\ell^3 - 2\pi a f_s \ell\right\} \le 0 \qquad (35)$$

[C] *Using a dipole moment of HF, which is =3.7 D=12.34×10^{-30}cm, the calculated electrostatic potential for a dipole pair is: V=-μ^2 /4πε$_o$ r^3=1.7×10^{-12} erg, and C=-ρ× (πa^2 V)=-ρ×3.012×10^{-28}erg /cm, where r= 2A and 2a=1.5A. If we let L=100A. and make use of: $\ell^* = L = \sqrt{C/3A}$ connection, where A=1.29×10^7 erg/cm^3 obtained previously for the stored elastic energy due to unusual torque term, then one finds ρ (↓↑)=--1.28×10^{23} #/cm^3, as the number of excess anti-align dipole pair per unit volume. The probably frequency of the pairs in the α-helical conformation having a length of L is given by P=ρ πa^{2}L=22.6#. Then the probably frequency of the pair per amino acid residue becomes Pre=P/11≅-2. This shows that two excess anti-align pairs are required to stabilize one amino-acid residue for 3.6$_{11}$ α-peptide. This high probability frequency is due to the selected very high shear modulus, G=1GPa. One order of magnitude reduction in G while keeping the arc length invariant one obtains a factor of ten reduction in the pair probability frequency P$_{re}$=-0.2. For this case, the electrostatic binding energy due to the excess anti-align dipole pairs for the whole helix conformation reduces to $\nabla_{\uparrow\downarrow}$=-2/3 C$\sqrt{C/3A}$ -1.6 eV, and 0.147 eV per amino acid residue (-3.95 Kcal/mol)[44].*

[d] *In our incoming paper, this precondition on the enclosing cage structure will be relaxed completely by taking into account of the quasi-free variations in the pitch height and the radius of the helical shape (i.e., λ will be now independent variable) while keeping its volume constant but flexible (isochoric) in order to simulate the unfolding process.*

In addition, with the following imposed constrains on the backbone skeleton:

$$\delta V_o(a\ell)\delta\left\{\pi a^2\ell\right\}=0,\ \delta\lambda=0 \tag{36}$$

Where δ is variation operator, `a' and are not independent variables, since they are constrained by the second equation above, which claims that the volume of the amino-acid skeleton $V_o(a\ell)=V_o$ is invariant quantity $\delta V=0$ under the isothermal $\delta T=0$ and isochoric conditions. Vo is the volume of the alpha peptide, which is assumed to be closed (no exchange of matter) and separated from the surroundings by conductive workless boundary conditions.

The above set of variables can be put into the independent variable form by defining a new function, $\Sigma(a\ell)$ which is subjected to extremal solutions such as

$$\delta\Sigma(a\ell)=\delta\{\nabla F(a\ell)+\chi V(a\ell)\}\le 0 \tag{37}$$

where *x* is the Lagrange Multiplier. We can then set the solution of the variational problem into the following format:

$$\delta\Sigma(a\ell)=\delta\nabla F(a\ell)+\chi\delta V(a\ell)=0 \text{ And } V(a\ell)=V_o \tag{38}$$

This yields two independent equations in terms of the partial derivatives of $\Sigma(a,\ell)$ with respect to $\{\ell,a\}$ independent variables. These may be put into the following form after some legitimate cancelations, where $\{\ell,a,\chi\}$ are unknown independent variables:

$$\partial\Sigma(a\ell)/\partial\ell=4G\lambda^2 a\ell^2-2f_S+\chi a=0,$$

$$\partial\acute{O}(a,\ell)/\partial a=4G\lambda^2 a\ell^2-3f_S+3\chi a=0$$

$$V=\pi a^2\equiv V_o \text{ constant} \tag{39}$$

The solutions above can be easily obtained, which results in $\chi=fs/2a$ from Eq. (ii) and (i), respectively: After some algebraic procedures, the following expressions for the extremal values associated with the stable length ℓ^* and radius a^* of the helical conformation can be obtained in terms of physicochemical system parameters:

$$\ell^*=\left(\frac{\pi}{V_o}\right)^{1/3}\left(\frac{3}{8}\frac{fs}{G\lambda^2}\right)^{2/3} \text{ and}$$

$$a^*=\left(\frac{\pi}{V_o}\ell^*\right)^{-1/2}\Rightarrow\left(\frac{\pi}{V_o}\right)^{-2/3}\left(\frac{3}{8}\frac{fs}{G\lambda^2}\right)^{-1/3} \tag{40}$$

Using above findings, the changes in the critical length and the radius with respect to the volume of the peptide can be calculated and plotted in Figure 13, which shows monotonic decrease in length but not radius with volume. The binding or extremal Helmholtz free energy can be obtained by substituting the calculated extremal values of the length and radius of the helical conformation into the expression for *F* (*a*, *ℓ*), which corresponds to a non-equilibrium stationary state. Then one reads:

$$E_b\equiv\nabla F_G\left(a^*,\ell^*\right)=\frac{4\pi}{3}G\lambda^2 a^{*2}\ell^{*3}-2\pi a^*\ell^* f_s \tag{41}$$

This expression can be further reduced to a form that involves only the internal physicochemical parameters of the system, such as $\{f_s,G,\lambda,V_o\}$, using explicit connections associated with $\left(a^*,\ell^*\right)$ in Eq. (A-7). This amounts to the following rigorous and compact expression after the arithmetic manipulation of the terms:

$$\nabla F_G\left(a^*,\ell^*\right)\Rightarrow E_b'(f_S,G,\lambda,V_o)=-\frac{3}{4}\left\{2\pi\left(\frac{\pi}{Vo}\right)^{-1/3}\left\{\frac{3f_S}{8G\lambda^2}\right\}^{1/3}f_S\right\} \tag{42}$$

It is remarkable that the expression between the curly braces is nothing but the critical value of the Helmholtz surface free energy, which was designated by $B^*\ell^*\Rightarrow(2\pi a^*\ell^* f_S)$, in our previous sections such as in Eq. (26), where we have had the following expression for the binding free energy; $\nabla F_G^*=-2/3\,B(B/3A)^{1/2}\Rightarrow -2/3\,B\ell^*$. This formula was obtained by assuming that the radius of the amino acid backbone is frozen, which violates the constant volume condition, but not necessarily the isochoric requirement. The difference between these two approaches is negligible in terms of the binding energy, as shown by numerical checking (δLnEb =1/12). Both mathematical approaches attempt to find the extremal state under different constraints, but from a mathematical point of view, the present approach is sounder, but still cannot address the unfolding scenario.

Figure 13. The Helmholtz binding free energy, E_b the length ℓ^* and the radius *a** of α-Peptide with a simple helical conformation at the stationary non-equilibrium state under the isothermal isochoric conditions. Here α-Peptide is in the folded state, which is subjected to the stored ``anomalous or unusual '' torsional deformation energy induced during the folding process that shows very small drop 0.021eV during the relaxation. There is also very small drop in the global

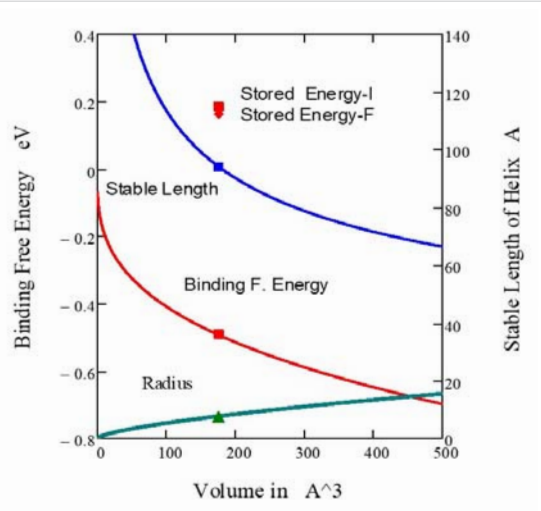

Figure 13: The Helmholtz binding free energy, E_b the length ℓ^* and the radius *a** of α-Peptide with a simple helical conformation at the stationary non-equilibrium state under the isothermal isochoric conditions. Here α-Peptide is in the folded state, which is subjected to the stored "anomalous or unusual" torsional deformation energy induced during the folding process that shows very small drop 0.021eV during the relaxation. There is also very small drop in the global Helmholtz free energy, 0.001 eV. Data: G = 23 MPa and fs = 20 erg/cm^2, and λ = 2.34 x 106 cm^{-1}. The marks on the line plots belong to the α-peptide characterized by the invariant volume of Vo = 1.767x10-22 cm^3.

Helmholtz free energy, 0.001 eV. Data: G = 23 MPa and fs = 20 erg/cm^2 , and λ = 2.34 x 106 cm-1. The marks on the line plots belong to the α-peptide characterized by the invariant volume of Vo = 1.767 x 10-22 cm^3.

If we take previously employed values for α-helix such as: a = 0.75A; Lo = 100A, which corresponds to Vo = 1.767 x 10-22 cm^3, and λ = 2.34 106 cm-1 in connection with the shear modulus as reported by Leon, et al. [42,43] G=2.3 x 108 dyne/cm^2 (23 MPa), and the Helmholtz specific surface free energy as fs = 73 erg/cm^2, we may obtain the following values (after subjected to the numerical relaxation procedure) for the radius, the length and the binding free energy, respectively, at the non-equilibrium stationary stable state: ac = 0.77A; Lc = 94A; Eb =-7.9 x 10-13 erg =-0.49 eV (-11.4 Kcal/mole), that corresponds to -0.044 eV (-1.0 Kcal/mole) per amino acid residue in 3.6_{11}, which has four distinct atomic species, respectively, (N,C',Cα,O) in its back- bone structure in addition to the two hydrogen atoms plus the radicals to make up the skeleton[e] [38].

Therefore, there are 11-13 HB bonds if one considers the N- and C-terminal capping. It is remarkable that the binding energy calculated here is almost equal to that previously obtained from the naïve approach to the stability problem, but the critical length reported as 93 A in the text was reduced to approximately 7%; at the same time, the radius showed an approximately 3% increase while keeping the volume perfectly constant, Vo = 1.767 x 10-22 cm^3. where $\delta V/V = 2\delta a/a + \delta l/l$.

According to the extensive spring mechanics studies conducted by Idiris, et al. [3] on α- helical polypeptide exposed to wide range of pH (0.3-0.8) environments, the unfolding energy, which is strongly correlated with the surface free energy term in our theory varies between 0.5 – 7.5 eV (pH-8.0) up to 7.5 - 55 eV(pH-3.0) depending upon the amount of extension, which varies from E = 1.25 nm up to – E = 25.0 nm during the AFM stretching experiments done on single (Glu)n –Cys chain n = 80, helicity = 80%). Their reported Young modulus was 3GPa, assuming that the length of the α-helix was L = 10 nm and the radius was 0.2 nm. Idiris, et al. [3] claimed that their findings are reasonable because they are in agreement, within a factor of two, with the theoretical calculation of Gang Bao from the GIT (personal communication). The present author believes that the original definition of Young's modulus, which is valid for linear Hookean solids or hyperelastic materials, cannot be used in the present case because their force-extension plot (F-E) shows strong nonlinearity, which can be represented by a second-order (quadratic) polynomial, as suggested by the functional length dependence of the unusual torque term obtained rigorously in this study. This behavior can also be observed in the unfolding energy versus elongation F-E plots from the study by Idiris, et al. [3] such as Figures 5,6. at high pH values. The bond-breaking energies were obtained from the α-helix (AH1), which is a domain from the 2 B segment of the vimentin intermediate filament.

Results and discussion

In the first part of the applications denoted by Section-V , the electromechanical stability of the strained helical confirmations is treated under isothermal isochoric and isobaric conditions. A special reference for the application of this theory to the α-peptide structure of amino acid complexes is given by employing two different irreversible thermodynamics methods according to the imposed constraints on the free variables to obtain a simple and manageable mathematical model. In our following paper [39] on the spontaneous unfolding of helical conformations, we introduce a more general relaxation approach using the Lagrangian multiplier method to solve the extremum problem. While dealing with the electromechanical stability of this highly complex and discrete atomic skeleton of peptides, we are still insisting on staying in the domain of the continuum approach. The most important outcome of the present naïve thermodynamic approach to the stability problem is the unique role of the interfacial Helmholtz free energy of the boundary layers enclosing and separating the peptide skeleton from its immediate internal and external aqueous solution environment, which may be characterized by a single electrochemical quantity, that is, the pH level. As far as the critical or non-equilibrium stationary stable arc length of the alpha-helical conformation is concerned, for isochoric isothermal systems, there is only one physicochemical parameter that plays a major role, which is the ratio of the surface (interface) Helmholtz free energy and the shear modulus of elasticity, namely, f_s/G.

In Section-VI, irreversible thermokinetics of helical conformation is formulated, where not only bulk Helmholtz free energy but also the surface Helmholtz free energy is taken into account for the spontaneous natural change in the global Helmholtz free energy, which pushes the system towards the non-equilibrium stationary state [6]. That hypothesis may be also justified by the Planck (1887) criterion [22] for isochoric isothermal changes for closed systems. That is also connected to the Prigogine's positive definite entropy production hypothesis as a special case: $\delta\nabla S_{in} = -\mathrm{T}^{-1}\delta\nabla F_G \geq 0 \;\forall\; \delta\mathrm{V}=0$, where equal sign for reversible (equilibrium) processes, and positive sign for the irreversible or natural processes.

In Section-VII, a variational formulation of the isochoric isothermal stability of the strained helical conformation is considered using rigorous mathematical formulation. Here, we clearly have a non-equilibrium deformation problem such

[e] Middleberg, et al. [43] reported values for Young modulus E=20-80 MPa (2-8x10^8 dyne/cm^2) and the interfacial tension as 73-120 (erg/cm^2) for a peptide film having 15 A thickness, and self-assembled at the air water interface.
Idiris A, Taufiq M, Ikai A. Spring Mechanics of α–Helical Polypeptide, Protein Eng. 13(11) : (2000) pp.763-770.

that the system, even in the absence of external tractions and body forces (with the exception of gravity), maintains its external form and internal integrity for a sufficiently long time.

Conclusion

1. In this work, we have demonstrated that the application of pure torsion to a circular bar generates not only a simple torque from the symmetric part of the deformation tensor but also a torque term obtained though the anti-self-conjugate part of that deformation tensor. This new unusual torque term originates from the non-vanishing shear force field directed along the tangential vector of the circumferences of the cylindrical wall surface.

2. The rigorous adaptation of this pure torsion problem for simple helical springs, which mimics the helical conformations of folded proteins such as α-peptides and DNA , resulted in very interesting findings, which are closely associated with the vorticity of the screw symmetric deformation tensor approaches zero, which means that the direction of the unusual torque term after a few precessions tries to align with the z-axis of the helix.

3. The behavior of the helical conformation under isochoric and isobaric conditions was analyzed and formulated using fundamental postulates of irreversible thermodynamics. Kinetic equations related to deviations from the non-equilibrium stationary state configuration are obtained, which show that the gradient of the unusual torsional elastic energy acts as the main driving force for the inherent stability.

4. It has been demonstrated that the main contribution to the mechanical stability of α-peptide 3.6_{11} cannot come alone from the electrostatic dipole-dipole interaction potential of the anti-align excess dipole pairs but also from the surface Helmholtz free energy, which is characterized by a binding free energy of -15.5 eV/molecule (-32.56 Kcal/mole) for an alpha-peptide composed of 11 amino acid residues with a critical arc length of approximately 10 nm, assuming that the shear modulus [40] is G=1GPa and the surface Helmholtz specific free energy density is fs=800 erg/cm^2. This result is in excellent agreement with the experimental observations of the AH-1 conformation of (Glu)n Cys at pH 8 by Idiris, et al. [1].

5. Irreversible thermodynamic treatment of the helical conformation provides a method for calculating not only the stationary state length but also the binding Helmholtz free energy under isochoric isothermal conditions. The critical length obtained in this work for the 3.6^{11} α-peptide is in excellent agreement with experimental findings of 10 nm at 275^o- 360 ^{0}C as the most abundant conformation size in nature for folded and extended states.

6. We have also provided quantitative arguments that one excess anti-aligned dipole pair per amino acid residue may be sufficient for the mechanical stability of α-helix conformations against the large stored torsional elastic deformation energy supplied during folding. The calculated binding Helmholtz free energy in the presence of two permanent anti-align electrostatic dipole pairs was found to be -0.37 eV assuming that G=23MPa for α-peptide 3.6^{11} having 11 amino acid residues, which is almost equivalent to the one obtained for the case where the surface Helmholtz free energy fs=23 erg/cm^2 functions as a stabilizer.

7. The present theory indicates that only two excess permanent anti-align dipole pairs for one α-Helical peptide molecule is requirement to stabilize the whole secondary structure of the protein that is exposed to heavy torsional deformation during the folding processes which amounts to 7.75 eV/molecule stored electrostatic energy compared to the interfacial Helmholtz free energy of -23.25 eV/molecule, which is exposed to hydrophobic environments.

8. The quantitative estimates relying on the available physico chemical-data [G=23MPa; fs=23 erg/cm^2] indicate that the stored torsional deformation energy because of folding process is about 4.27 kcal/mole (0.185 eV/molecule) for the whole α-helix structure having 11 amino acid residue and 11-13 HB, which is exactly the 2/3 of the surface free energy (2π a fs Lo), which amounts to 0.667 eV. This ratio was also predicted using the naïve theory presented in the previous section. These figures are also very close to the case in which one has two anti-aligned dipole pairs that act as stabilizers.

Data availability statement

Data for the experimental points were extracted directly from the graphics, as shown in Figures 5,6. of a published work by *A*. Idiris, M. Taufiq, A. Ikai, (2000), ``*Spring Mechanics of α–Helical Polypeptide*, Protein Eng. 13(11) : (2000) pp.763-770. This work is cited as Reference [38,41,42] in our previous study [21]. The data are openly available-in: https://www.google.com.tr/search?q=A.+Idiris,+M.+Taufiq,+A.+Ikai,+Spring+Mechanics+of+%CE%B1%E2%80%93Helical+Polypeptide,+Protein+Eng.+13(11)+:+(2000)+pp.763-770.

Acknowledgment

The author wishes to thank Professor Walter F. Schmidt of the Agricultural Research Service, USA, who provided valuable advice and inspired us to show interest in the energetic and macrostatic stabilities of the helical conformations of peptides. We also extend our gratitude to Prof. Dr. Ersin Emre Oren, Department of Biomedical Engineering, and Dr. Ömer Refet Cayhan, and Mr. Erhan Gürpinar, Department of Nanotechnology and Materials Science, TOBB University of Economics and Technology, Ankara, for their helpful discussions on this work. The author would also like to thank to Dr. Aytaç Çelik of Department of Materials and Metallurgical Engineering, Sinop University, and the Academic Members of the Department of Metallurgical and Materials Engineering

of Middle East Technical University, Ankara, Turker, for their helpful discussions on the theory of non-Hookean elasticity part of this extensive manuscript.

Ethical compliance: All procedures performed in this study involving human participants were in accordance with the ethical standards of the institutional and/or national research committee and with the 1964 Helsinki Declaration and its later amendments or comparable ethical standards.

Conflict of interest declaration: The authors declare that they have no affiliations with or involvement in any organization or entity with any financial interest in the subject matter or materials discussed in this manuscript.

Author contributions: The author was solely responsible for all aspects of this work, including the conceptualization, methodology, investigation, data analysis, and writing of the manuscript.

References

1. Saint-Venant JCB. Mémoire sur la torsion des prismes. Mém Divers Savants. 1855;14:233-560.
2. Kumar P. Densities, viscosities, and speed of sound and other acoustic parameters of L. Alanine in aqueous alcohols at different temperatures. Rasayan J Chem. 2012;5(3):424-431. Available from: https://www.researchgate.net/publication/289831127_Densities_viscosities_and_speed_of_sound_and_other_acoustic_parameters_of_L_Alanine_in_aqueous_alcohols_at_different_temperatures
3. Idiris A, Taufiq M, Ikai A. Spring mechanics of α–helical polypeptide. Protein Eng. 2000;13(11):763-770. Available from: https://doi.org/10.1093/protein/13.11.763
4. Timoshenko S, Goodier JN. Theory of elasticity. New York: McGraw-Hill Book Co.; 1951;259:391.
5. Landau LD, Lifshitz EM. Theory of elasticity. Oxford: Pergamon Press; 1981;68.
6. Ogurtani TO. Variational formulation of irreversible thermodynamics of isochoric and isobaric systems. 2015. Available from: https://www.researchgate.net/publication/281973641_Variational_Formulation_of_Irreversible_Thermodynamics_of_Isochoric_and_Isobaric_Systems
7. Rice JR, Ducker DC. International journal of fracture mechanics. 1967;3:19-27.
8. Eshelby JD. In: Seitz F, Turnbull D, editors. Solid state physics. Vol. III. New York: Academic Press; 1956;79-144. Available from: https://shop.elsevier.com/books/solid-state-physics/seitz/978-0-12-607703-2
9. Weatherburn CE. Elementary vector analysis with application to geometry and mechanics. London: G. Bell and Sons, Ltd.; 1955;101.
10. Weatherburn CE. Advanced vector analysis with application to mathematical physics. London: G. Bell & Sons; 1954; 142.
11. Fung YC. Foundations of solid mechanics. Englewood Cliffs, New Jersey: Prentice-Hall; 1965;158:167:478. Available from: https://www.scribd.com/doc/150034924/Foundations-of-Solid-Mechanics-PH-1965-Fung-Y-C
12. Landau LD, Lifshitz EM. Mechanics. 3rd ed. Oxford: Pergamon Press; 1976;109.
13. De Saint-Venant. Mémoire sur la torsion des prismes. Mém Savants Étrangers. 1855;14:1-56. Available from: https://babel.hathitrust.org/cgi/pt?id=hvd.32044091959866&seq=1
14. Boley BA. Some observations on Saint-Venant's principle. In: Proceedings of the 3rd U.S. National Congress on Applied Mechanics. Providence, RI; 1958;259-64.
15. Love AEH. A treatise on the mathematical theory of elasticity. Cambridge: Cambridge University Press; 1927;571.
16. Young YC. Foundations of solid mechanics. Englewood Cliffs, New Jersey: Prentice Hall; 1965;306.
17. Lamb and Clapeyron. See: Crelle's J. 1830;7:19-831.
18. Moss GP, Working Party of the IUPAC-IUB Joint Commission on Biochemical Nomenclature. 1989.
19. Göhner O. Ingenieur-Archiv. 1930;1:619. 1938;9:355.
20. Timoshenko S, Goodier JN. Ibid. 1951;306.
21. Ogurtani TO, Oren EE. Mesoscopic irreversible thermodynamics of morphological evolution kinetics of helical conformation in bioproteins "DNA" under the isothermal isobaric conditions. Ann Biomed Sci Eng. 2020;1-11. Available from: http://dx.doi.org/10.29328/journal.abse.1001008
22. Ogurtani TO. Mesoscopic irreversible thermodynamics of alpha polypeptides [DNA] under various constraints: special reference to the simple spring mechanics. AIP Adv. 2024;14(2). Available from: https://doi.org/10.1063/5.0183144 .
23. Truesdell C. Thermodynamics of deformation. In: Donnelly RJ, Herman R, Prigogine I, editors. Non-equilibrium thermodynamics: variational techniques and stability. Proceedings of Symposium; University of Chicago; 1965. p. 101-14. Chicago: University of Chicago Press; 1966; 102. Available from: https://books.google.co.in/books/about/Non_equilibrium_Thermodynamics.html?id=harvAAAAMAAJ&redir_esc=y
24. Ogurtani TO, Çelik A, Ören EE. Generic role of the anisotropic surface free energy on the morphological evolution in a strained-heteroepitaxial solid droplet on a rigid substrate. J Appl Phys. 2010;108:103516. Available from: https://doi.org/10.1063/1.3512970
25. Shelby SM. CRC standard mathematical tables. Cleveland, Ohio: CRC Press; 1973;412:Eq-18.
26. de Groot SR. Thermodynamics of irreversible processes. Amsterdam: North-Holland Publishing; 1961;27. Available from: https://www.scirp.org/reference/referencespapers?referenceid=120488
27. Prigogine I. Thermodynamics of irreversible processes. New York: Interscience Publishing; 1955;75.
28. Qin Z, Kreplak L, Buehler MJ. Nano mechanical properties of vimentin intermediate filament dimers. Nanotechnology. 2009;20:425101. Available from: https://doi.org/10.1088/0957-4484/20/42/425101
29. Hiltpold A, Ferrarai P, Gsponer J, Caflish A. Free energy surface of the helical peptide Y(MEARA)6. J Phys Chem B. 2000;104(43):10080-6. Available from: https://pubs.acs.org/doi/pdf/10.1021/jp002207k
30. Middelber PJ, He L, Dexter AF, Shen HH, Holt SA, Thomas RK. The interfacial structure and Young's modulus of peptide films having switchable mechanical properties. J R Soc Interface. 2008;5:47-54. Available from: https://doi.org/10.1098/rsif.2007.1063
31. Guggenheim EA. Thermodynamics: an advanced treatment for chemists and physicists. Amsterdam: North-Holland; 1956;410-5.
32. Pauling L, Corey RB, Branson HR. The structure of proteins: two hydrogen-bonded helical configurations of the polypeptide chain. Proc Natl Acad Sci U S A. 1951;37(4):205-11. Available from: https://doi.org/10.1073/pnas.37.4.205
33. Hol WGJ. The role of the α-helix dipole in protein function and structure. Prog Biophys Mol Biol. 1985;45:149-95. Available from: https://doi.org/10.1016/0079-6107(85)90001-x
34. Ackbarow T, Chen X, Sinan K, Buehler MJ. Hierarchies, multiple energy barriers, and robustness govern the fracture mechanics of α-helical and β-sheet protein domains. Proc Natl Acad Sci U S A. 2007;104(42):16419-24. Available from: https://doi.org/10.1073/pnas.0705759104

35. Bell GI. Model for the specific adhesion of cells to cells. Science. 1978; 200:618-27. Available from: https://doi.org/10.1126/science.347575

36. Bernstein FC, Koetzle TF, Williams GJB, Meyer EF, Brice MD, Rodgers JR, et al. The Protein Data Bank: a computer-based archival file for macromolecular structures. J Mol Biol. 1994;112:535-542. Available from: https://doi.org/10.1016/s0022-2836(77)80200-3

37. Hildebrand FB. Methods of applied mathematics. Englewood, NJ: Prentice Hall; 1961;122.

38. Leon EJ, Verma N, Zhang S, Lauffenburger DA, Kamm RD. Mechanical properties of a self-assembling oligopeptide matrix. J Biomater Sci Polym Ed. 1998;9:297-312. Available from: https://doi.org/10.1163/156856298x00668

39. Middelber PJ, He L, Dexter AF, Shen HH, Holt SA, Thomas RK. The interfacial structure and Young's modulus of peptide films having switchable mechanical properties. J R Soc Interface. 2008;5:47-54. Available from: https://doi.org/10.1098/rsif.2007.1063

40. Middleberg, et al. Reported values for Young's modulus E = 20-80 MPa (2-8 x 10^8 dyne/cm^2) and the interfacial tension as 73-120 erg/cm^2 for a peptide film having 15 Å thickness, self-assembled at the air-water interface.

41. Ogurtani TO, Oren EE. Mesoscopic irreversible thermodynamics of morphological evolution kinetics of helical conformation in bioproteins "DNA" under the isothermal isobaric conditions. Ann Biomed Sci Eng. 2020;1-11.

42. Ogurtani TO. Mesoscopic irreversible thermodynamics of alpha polypeptides [DNA] under various constraints: special reference to the simple spring mechanics. AIP Adv. 2024;14(2). Available from: https://doi.org/10.1063/5.0183144